Status of the Longitudinal Emittance Preservation at the HERA Proton Ring in Spring 2003

Elmar Vogel
Deutsches Elektronen-Synchrotron DESY, Hamburg, Germany

DESY Report No. DESY-HERA-03-03, 2003

Abstract

At the upgraded electron proton collider HERA (HERA II), the proton bunch length is relevant for the achievable luminosity. This is due to the enhancement of the effective cross section at the interaction region when the beta function and the bunch length have comparable magnitude, 'hour-glass-effect' [1].

Several beam dynamical effects, such as beam loading transients at injection, coupled bunch oscillations during ramping and technical problems lead to a longitudinal emittance dilution. These effects can now be routinely observed and are permanently recorded with the new fast longitudinal diagnostics system (FLD). To reduce the bunch length, we began to implement several measures, such as RF amplitude modulation, introducing Landau damping at low energy and debugging the frequency controls and RF systems. In this report, the actual status of these activities will be given.

Contents

1 Introduction

At HERA II, strong focussing, superconducting magnets inside the detectors H1 and ZEUS lead to smaller beam cross sections at the interaction regions and hence to higher luminosity. Due to the strong focussing, the beta function and the bunch length are comparable in magnitude. This enhances the effective cross section, 'hour-glass-effect' [1]. A reduction of the bunch length would result in smaller effective cross sections and so further increase the luminosity.

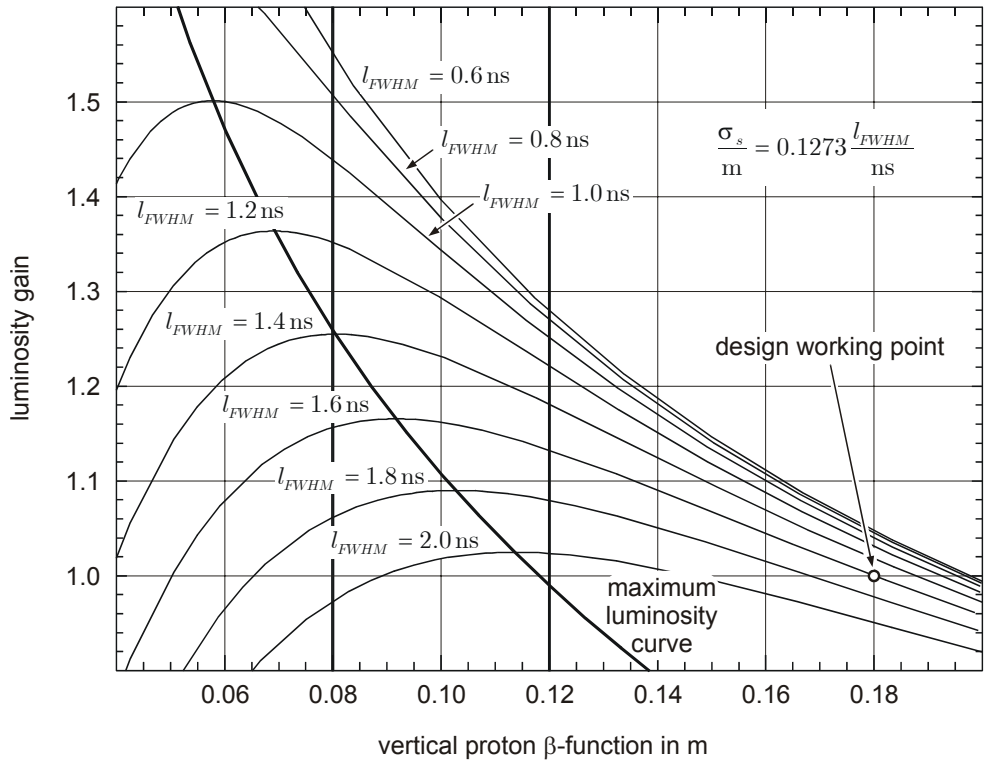

Figure 1.1: Dependence of the HERA II luminosity gain on the vertical proton β-function and the bunch length. ($\mathcal{L}_{design} \approx 7 \cdot 10^{31}\,\frac{1}{\mathrm{cm^2\,s}}$)

Figure 1.1 shows the luminosity gain, scaled from the design value, as a function of the vertical proton β-function and the bunch length[1]. The geometrical aperture of the proton storage ring, especially in the half quadrupole magnets with mirror plates, gives a lower limit for the vertical proton β-function. For commissioning $18\,\mathrm{cm}$ was chosen to have enough safety margin. The safety margin from the last HERA operation period, using the old optics, allow $12\,\mathrm{cm}$. A further reduction is a challenge, the lowest possible limit seems to be $8\,\mathrm{cm}$ [2].

Typical FWHM bunch lengths after injection (40 GeV) into 52 MHz buckets are between $2.4\,\mathrm{ns}$ and $3.5\,\mathrm{ns}$. Bunch lengths at low energy above $2.4\,\mathrm{ns}$ are caused by beam loading transients during injections and beam oscillations which could be driven by the 52 MHz RF cavities, or by their control loops. During acceleration to 920 GeV, the bunch length reduces to $1.6\,\mathrm{ns}$ due to mainly the compression by an additional 208 MHz RF system. One would theoretically

[1] Here we quote bunch length in the time domain.

expect a bunch length of $l_{920\,\mathrm{GeV}} \approx 0.27\, l_{40\,\mathrm{GeV}}$ i.e. ≈ 0.6 ns at high energy from a bunch length of 2.4 ns at low energy. This is mainly prevented by coupled bunch oscillations during the ramp.

With the new Fast Longitudinal Diagnostic (FLD) system we are able to observe and record all these effects. Furthermore we have an on-line check, whether particular measures suppress them and whether they are sufficient to preserve the longitudinal emittance. In this report, the observed and examined emittance dilution effects at injection and during acceleration are presented and the actual status of the measures taken is discussed.

High energy protons stored in HERA, which are not trapped in the RF buckets are called 'coasting beam'. This beam complicates the data taking at experiments examining low angle scattering, such as the Very Forward Proton Spectrometer (VFPS) of H1, or the using the beam halo for collisions with a fixed target, HERA-*B*. Systematic examination of coasting beam production at high energy and measures to reduce the production rate are at an initial stage. Some first results are presented.

2 Data Acquisition and Archiving

In this chapter, the current features of the Fast Longitudinal Diagnostics (FLD) are presented from the view of a user. The underlying principles have been described in detail in [3]. In contrast to the previous work, the recent period of development was dominated by software development to integrate the system as a standard tool into the HERA control system and to make it comfortable and easy to use. The sophisticated data acquisition and archiving software was written by Hong Gong Wu[1], whereas Victor Soloviev[2] developed the comfortable display program.

2.1 Measured Values

At the Fast Longitudinal Diagnostics System (FLD) the expression 'Fast' means that the phase, length and intensity of each single bunch are recorded within the time subsequent bunches pass a resistive gap monitor. In practice, this is equivalent to a simultaneous recording of these parameters from all proton bunches in HERA. Furthermore, the system records RF transients in all six cavities. These transients are built up by the beam loading and the RF fast feedback loops, installed to suppress the beam loading. Accelerating cavity voltages and the phasing between the two RF frequencies of the proton ring, 52 MHz and 208 MHz, complete the measured data.

On account of the limited memory size on the ADC boards, the raw data is recorded for a certain time period before reading the memory out. After preprocessing this data, it is stored on a local hard disc. By setting particular parameters in the FLD timing hardware, the time period can be adjusted in steps between 0.14 seconds and 4.5 seconds. This corresponds to the different sampling rates of single bucket positions every 13th, 26th, 52th, 104th, 208th and 416th revolution. One record requires 4 Mbyte. All calibration and conversion factors used are also stored, in order to have the possibility of re-calibrating the data for later off line analysis. In addition, each record contains so called 'global variables', such as the accelerator energy, DC-current, status of phase loops and the longitudinal profile of a single bunch ('CMFL' or 'Lopez Monitor' at DESY).

The calculation power of the VME CPU used allows one record to be taken every 11 seconds. During injection, acceleration and one hour after high energy is reached, the system takes records within this interval. Afterwards, the time intervals are increased to 3 minutes and 40 seconds. Without beam, the data recording is stopped.

2.2 Front End Computer

A 'Front End Computer' (FEC) is a data acquisition computer which acquires and preprocesses raw data, taken from diagnostics hardware. The software processing this data at a FEC is called 'server'. A server also places the data at the users disposal, whereas the access takes place over the network. Display programs are running at the consoles in the accelerator control room (BKR) and selected computers in the laboratory offices. The software layer between them and

[1] from DESY group MST

[2] from DESY groups MPY respectively MST

the servers is at HERA the TINE (Three-fold Integrated Network Environment) protocol [4]. The whole software containing the servers the display programs and the layers between is called ‘control system’.

In the case of the FLD the FEC consists of an industry standard VME crate containing an AMD CPU with 330 MHz and a local IDE hard disc with about 30 Gbyte of capacity for intermediate data storage. Hard discs according to the IDE standard are not optimal, since our average data throughput is about 30 Gbyte in four days and we operate 24 hours per day. We already crashed hard discs. The use of hard discs according to the SCSI standard is in preparation. After testing several operating systems, the actual one used is the LINUX distribution Debian 3.0.

The raw data is sampled by five VME ADC boards each containing eight ADC channels, with a digital bandwidth of 10.6 MHz and an analog bandwidth of about 60 MHz. The boards used have been developed by DESY-ZEUTHEN for use at the Tesla Test Facility (TTF) and its successors [5]. Four ADC boards are used for the FLD standard data acquisition mode and one is installed for long time observations of single bunches as needed for high sensitive beam spectrum and beam echo measurements.

To supply the ADC board with clock and trigger signals with low jitter, the FLD also contains a ‘timing’-crate, developed by the DESY group FEA. In this unit, ECL gate arrays count 208 MHz RF waves to generate among others bunch clock signals. Several FPGA (field programmable gate array) units provides trigger signals by counting the clock signals. Delay lines allow the clock signals to be shifted for each ADC board in steps of 500 ps independently. One can remotely switch and control the timing modules via IO interfaces. For this purpose a VME IP-Digital carrier board from Green Spring Computers is installed, equipped with IP-Digital I/O IndustryPacks.

A tolerable access time to the data is guaranteed by an exclusive 100 Mbit/s network connection to the next router in the computer network.

2.3 Data Archiving

The ADC boards cause interrupt requests on the VME bus when a data record has been taken. This forces the data acquisition server to fetch the raw data, preprocess it and store it on the hard disc. Display programs only access this data record via a second server, called ‘archive server’. In this way, the data acquisition can not be disturbed by an increasing demand from display programs.

Two chron-jobs are running at the FEC. One prevents overrun of the local hard disc by deleting the oldest records when the disc is 90% full. The other combines together data records in packages of about 300 Mbyte as zip-files. These packages are copied to the DESY tape system ‘dCache’ [6] to give a durable archive. Our philosophy is to store as much data as possible to allow off line analysis without restrictions. Such restrictions are always caused by a preliminary selection of events for storage. We need more memory, but it turned out, that we are therefore able to examine successfully malfunctions occurring at HERA only once or twice a week during standard operation.

While the FEC is taking a data record every 11 seconds, the CPU has no time to generate zip-files in parallel. Therefore, the chron-job for storing data at the dCache first checks the status of the data acquisition server and only takes action when the server is acquiring data in larger time intervals or is idle.

Data records already deleted at the FEC but stored at the dCache can be obtained from a second archive server also running on a LINUX PC called ‘archive PC’. In addition to the archive server on the FEC, this server checks whether a particular record is actually stored on

the archive PCs hard disc in case there is an request for it. If the record is not available, the data package containing it, is copied back from the dCache, unzipped and the record supplied to the requesting user. This server is still under construction.

The archive PC also has an exclusive 100 Mbit/s network connection to the next router for tolerable access times.

2.4 Data Representation

For data representation in the control room and the laboratories offices, a comfortable display program was developed. It has two operation modes, figure 2.1. In the live mode it always

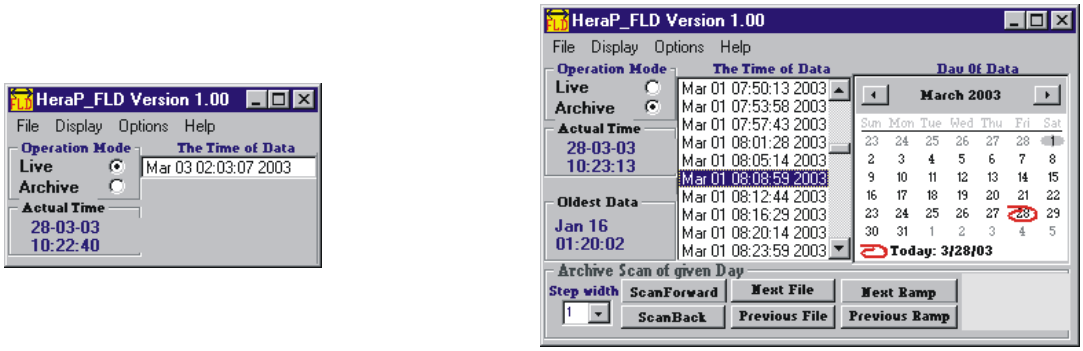

Figure 2.1: The FLD main window for the two different operation modes, the live mode and the archive mode. In the archive mode the window shows a calendar for choosing the time interval one is interested in.

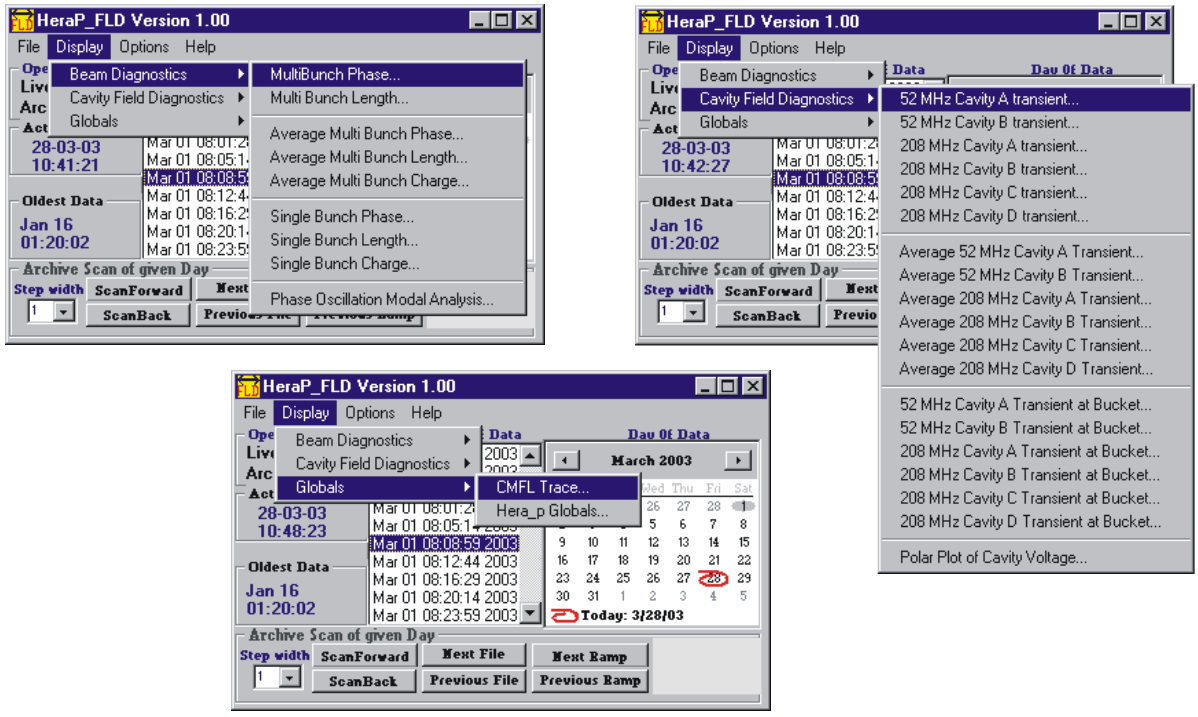

Figure 2.2: At the moment, 30 displays for the presentation and analysis of different aspects of a dada record are realized.

presents the newest record from the FECs hard disc. The archive mode shows a small monthly calendar, where a user can choose one day or several days in which he is interested. The time stamps of all available data records during the chosen period are then presented in a scroll box. By clicking on a certain time, the corresponding data record are presented. Furthermore, some simple data navigation possibilities are implemented, such as searching for start times of ramps. Pressing the scan forward or the scan backward button forces the program to present one record after the other, like a movie, starting at the actual presented record.

At the moment, there are 31 displays implemented for the presentation and analysis of the data in various ways. They can be switched on by choosing them via menus, see figure 2.2.

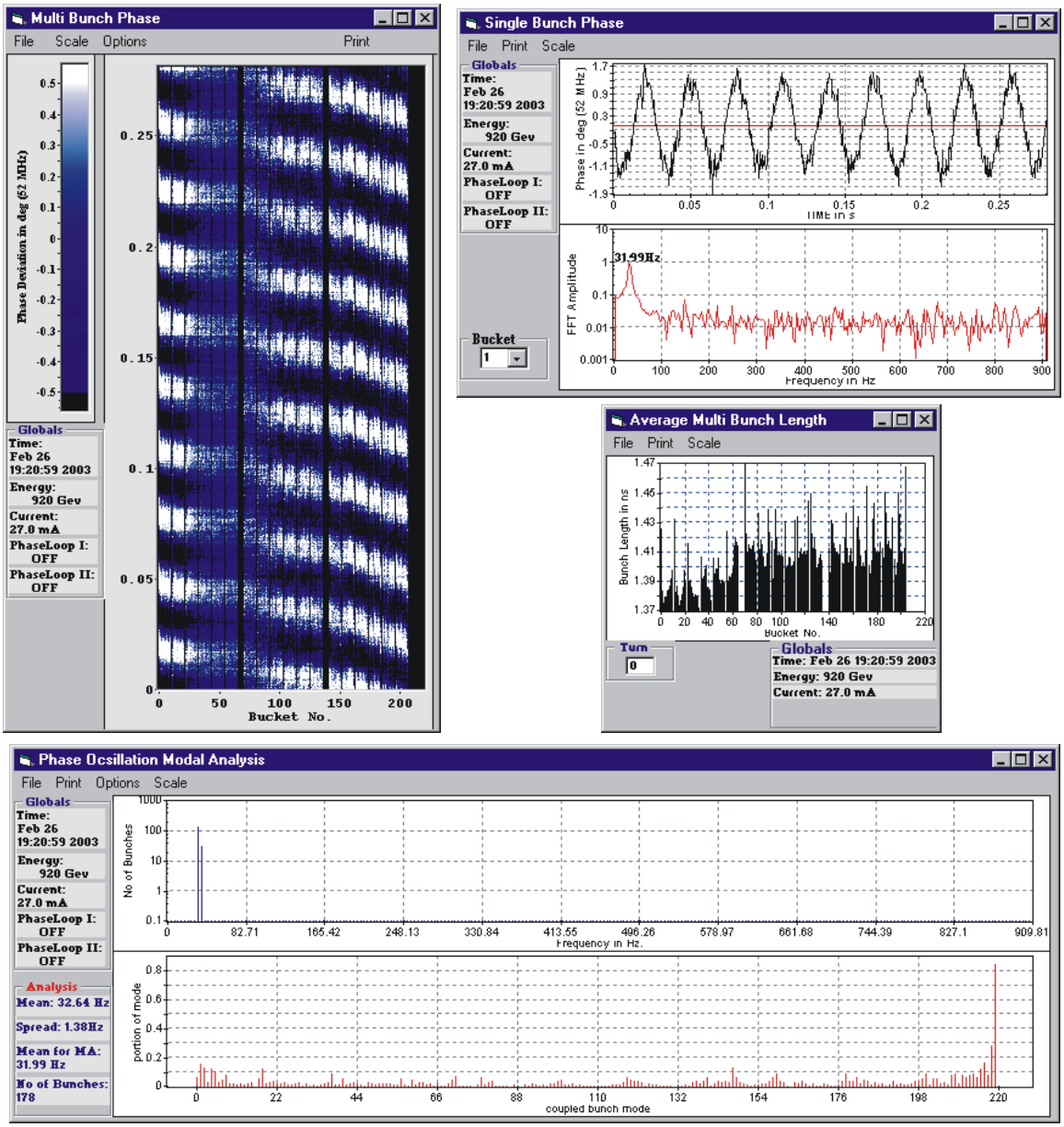

Figure 2.3: Some of the available displays to present and analyze FLD beam data.

Figure 2.3 shows some of the available displays for the presentation of beam data. For example, the 'Multi Bunch Phase' display shows, using a color scale, the phase oscillations of all bunches together. With some practice one may recognize immediately the longitudinal state of the beam. The 'Single Bunch Phase' display shows the bunch oscillation at the selected

bucket together with the FFT of this oscillation. The result of the steady state coupled bunch modal analysis, described in [3], is presented in the 'Phase Oscillation Modal Analysis' display. 'Average' displays are available for the presentation of the mean values of bunch phases, length and intensities. The values are calculated by averaging all values, contained in a data record, for each bucket position separately.

Figure 2.4 shows some displays for the presentation of cavity data. In the 'Average Cavity

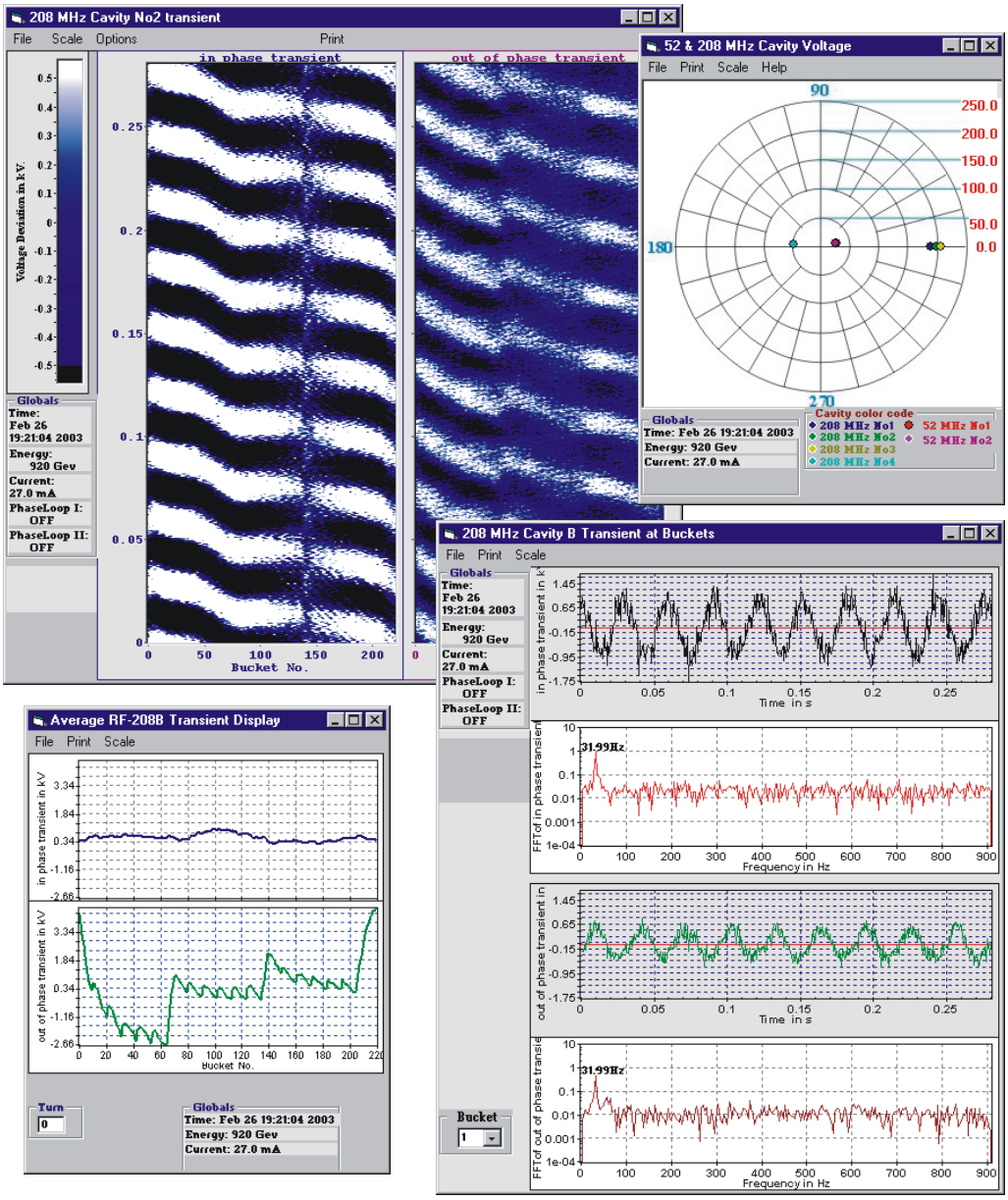

Figure 2.4: Displays to present and analyze cavity data.

Transient' display, the average steady state between beam loading and its suppression due to the fast feedback loops is presented. The 'Cavity Transient' display show the deviation from this average for the time at which the data record was taken. With the 'Transient at Bucket' displays, one can select one bucket position to examine the deviation from the average voltage a bunch at this position will see. A polar plot of the cavity voltages time averaged over all buckets is given in the '52 & 208 MHz Cavity Voltage' display.

We will not discuss here all features of the displays with respect to the different scaling

possibilities such as auto-scale, fixed scale, linear and logarithmic for FFT and so forth. A lot of these features should be self-explanatory. Choosing the print menu a user can send the display to a printer or even to the electronic HERA logbook.

For off line analysis, we also implemented the possibility to export the data, actually presented in a display, as a csv-file. Standard spread sheet programs import such files directly. Figure 2.5 shows this possibility using the 'Bunch Charge' display.

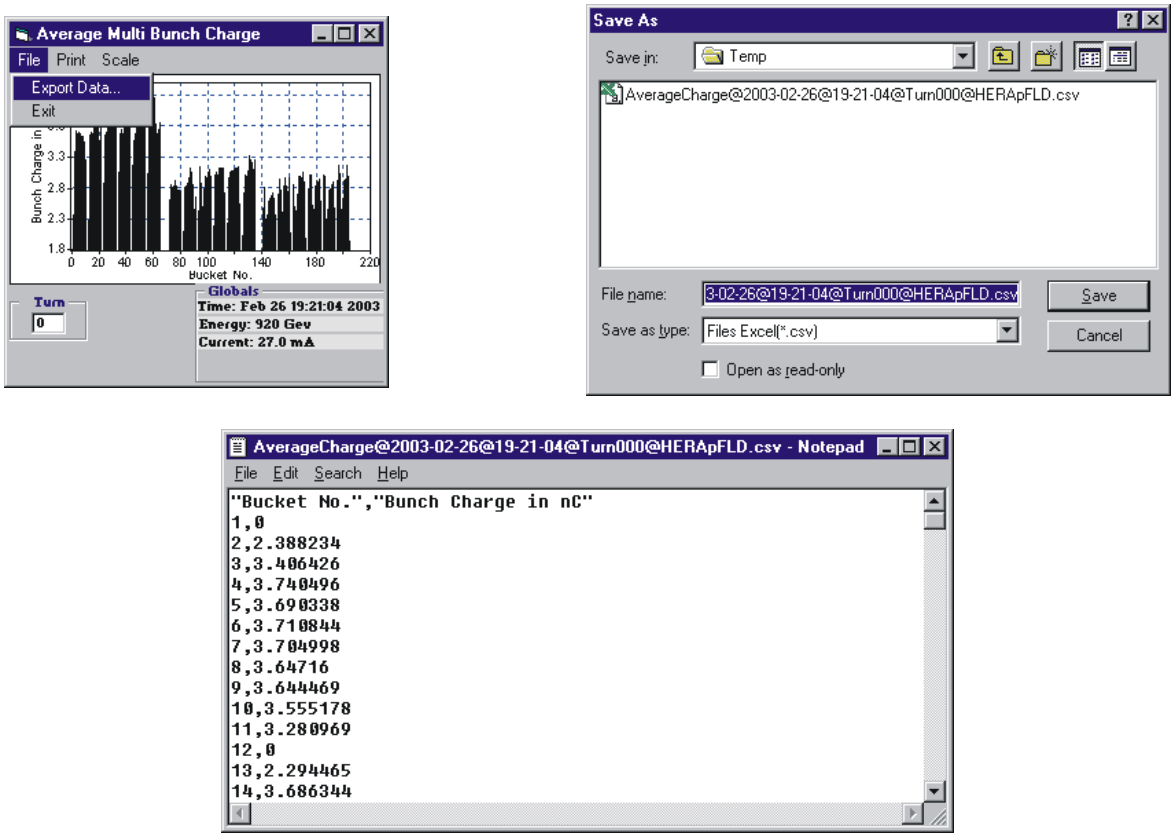

Figure 2.5: Choosing 'Export Data' in the 'File' menu opens a 'Save As' dialog box to change the recommend file name and path. The exported data is stored as a csv-file.

The FLD display program supports the user in post mortem analysis. He has only to switch the program into archive mode. Development of the display program is also uncoupled from accelerator operation. One can develop new displays even during shutdown periods by accessing archived data.

3 Observed Emittance Dilution Effects

In this chapter, we will discuss the most prominent emittance dilution effects, observed at the HERA proton ring. After suppressing these effects, additional effects may come to light. They are not yet considered.

3.1 Injections

The preservation of the longitudinal proton bunch emittance during the transfer from the pre-accelerator PETRA to HERA require the so called bunch rotation. The expression 'rotation' means that the bunch distribution is rotated in the PETRA phase space before the transfer, to match with the HERA buckets. This is done by changing every quarter synchrotron cycle the amplitude of the PETRA RF in steps. After each voltage change, the bunch rotates even more in phase space, observed as bunch length oscillation. But, this also dilutes the emittance. The optimum timing for transferring short bunches with low emittance is after three quarter synchrotron oscillations. The whole process is adjusted to result in matched bunch distributions in the HERA buckets [7].

As long as one transfers only one bunch from PETRA to HERA the bunch rotation results, in principle, in an ideal bucket matching. If there are already bunches inside HERA, either previous ones from an actual transferred train or from already stored bunch trains, they modify subsequent bucket potentials by beam loading. For subsequent bunches the bucket matching is no longer ideal, resulting in bunch oscillations and an increase of the longitudinal emittance. Furthermore, new injected bunches also cause beam loading acting on already stored bunches. All these transient effects together lead to an increase of the longitudinal emittance.

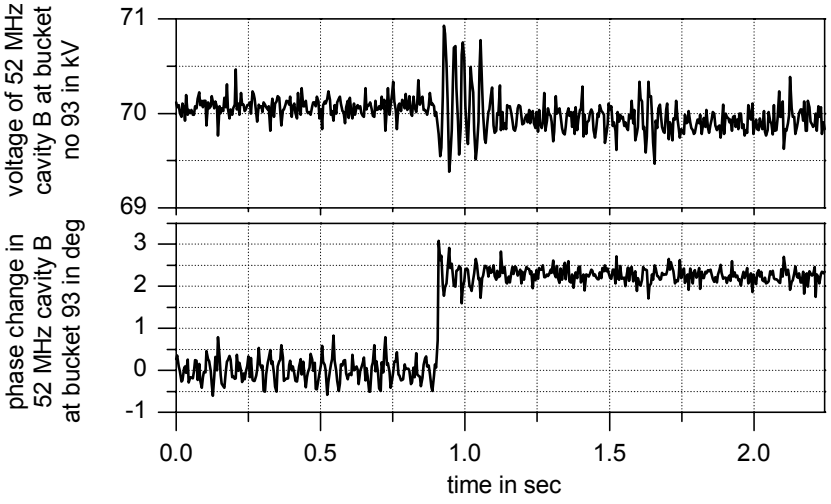

Figure 3.1: Transient changes of the RF in the 52 MHz cavity B due to the injection of the third bunch train (24th February 2003 at 00:08:10).

Figures 3.1 to 3.3 show the effect of the injection of 23 mA protons in a train of 40 bunches into HERA, when 45 mA in 80 bunches are already stored. The figures show the changes at

the arbitrary chosen bucket position no 93. Figure 3.1 and 3.2 present the transient changes of the RF voltages in the second 52 MHz cavity and the first 208 MHz cavity. The other cavities behave similary. The RF transients shown cause a phase oscillation of the bunch at position 93 resulting in a bunch lengthening and a loss of intensity, as shown in figure 3.3.

Aside, the particular fill pattern of three times 40 bunches was used to check, whether one can reach higher integrated luminosity with lower background in the experiments H1 and ZEUS as compared to the normal fill pattern of tree times 60 bunches. This divergence from the normal operation makes no fundamental difference in view of the beam loading effects shown.

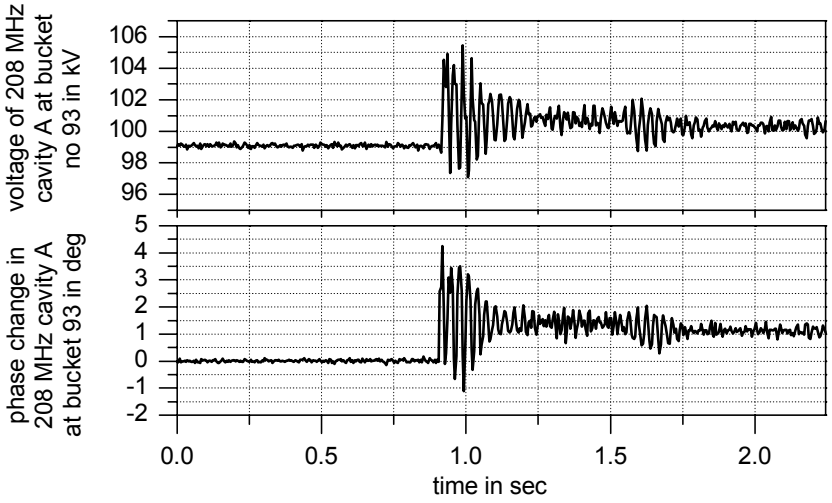

Figure 3.2: Transient changes of the RF in the 208 MHz cavity A due to the injection of the third bunch train.

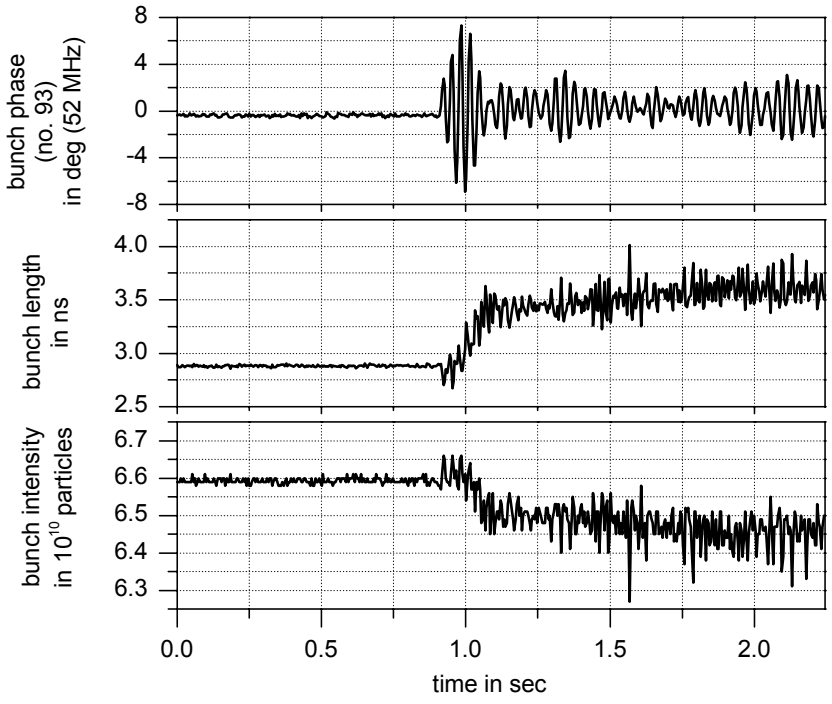

Figure 3.3: Oscillation of the already stored bunch at position 93, increase of its length and the loss of intensity due to the injection of the third bunch train.

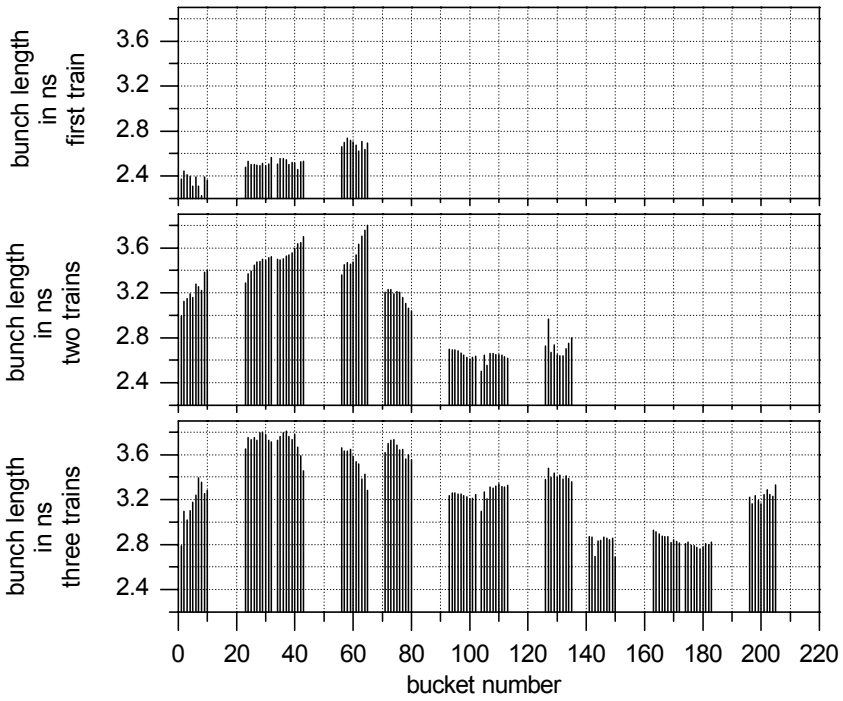

Figure 3.4: Bunch length development due to transient beam loading, caused by subsequent injected trains of 40 bunches each. The beam current after the last injection was 69 mA. Data from 24th February 2003 starting at 00:00 AM.

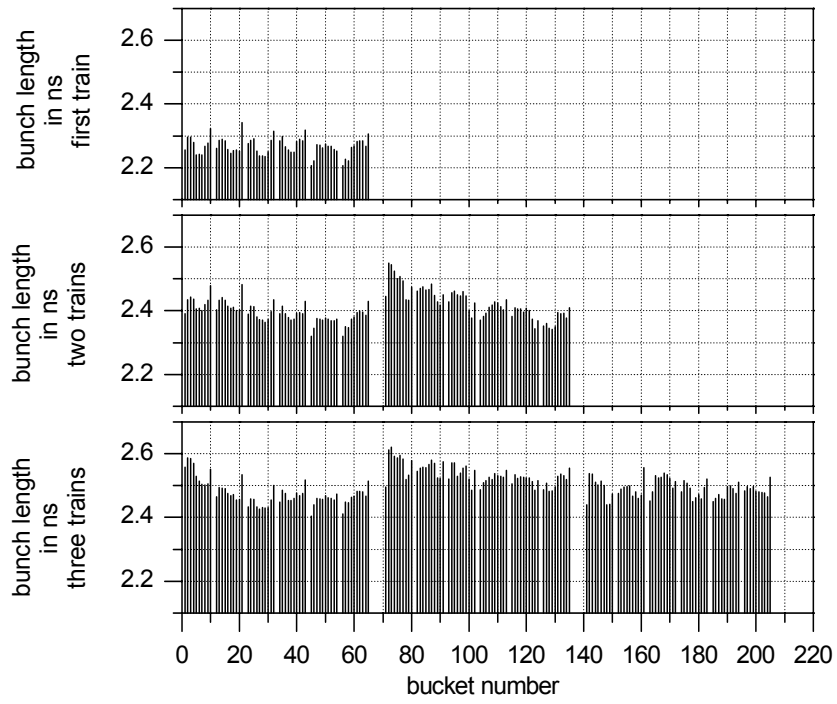

Figure 3.5: Bunch length development due to transient beam loading, caused by subsequent injected trains of 60 bunches each. The beam current after the last injection was 32 mA. Data from 16th January 2003 starting at 01:20 AM.

The bunch lengthening during the subsequent injection of three trains, each containing 40 bunches, is shown in figure 3.4. Figure 3.5 shows the case when trains of 60 bunches are injected.

Long bunches at the start of the acceleration normally lead to side-bunches in the neighboring 208 MHz buckets at high energy, this mean at the positions ± 5 ns from the bunch center. This is due to the bunch being too long for a proper transition from the initial 52 MHz potential into the 208 MHz potential. An extreme example is shown in figure 3.6, where a bunch with an initial length of 4.7 ns at low energy forms neighboring bunches during acceleration to high energy. The bunch length of 4.7 ns corresponds to a longitudinal emittance of 190 meVs at low energy.

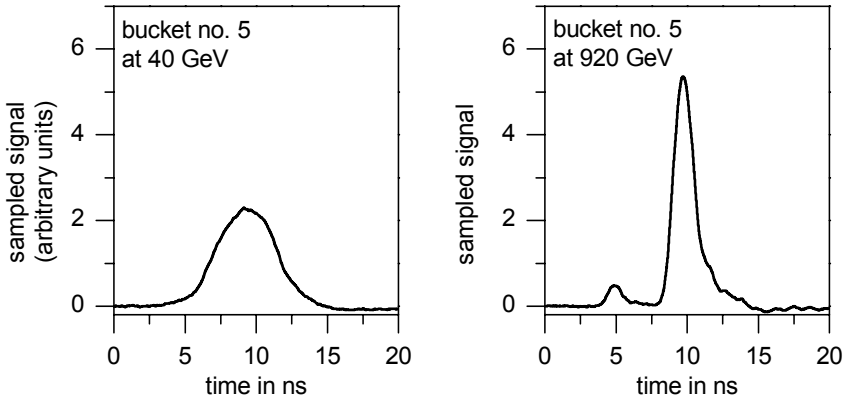

Figure 3.6: CMFL trace of a 4.7 ns long bunch at 40 GeV. Its length is reduced to 1.7 ns at 920 GeV. But, 5 ns in front of it, an additional bunch was formed (23. February 2003 02:02 PM).

Side-bunches seriously interfere with the data taking in the experiments H1, ZEUS and HERA-B.

3.2 Low Energy and Ramp up to 70 GeV

During the last HERA run period, we observed strong coherent beam oscillations at low energy with coupled bunch mode number $l = 0$. This means, all bunches oscillated in phase as figures 3.7 and 3.8 show. Reaching 70 GeV, these oscillations disappeared.

In May 2002, such oscillations were not visible, unfortunately we no longer have stored FLD data from this time since the FLD was still in an early development state. Nevertheless, even older data from HERA before the upgrade (HERA I), taken in 2000 with a test software, also shows no comparable oscillations, even with four times higher beam current, figure 3.9.

Already at the time of the first observation of these oscillations in July 2002, we had the suspicion that a technical malfunction in the 52 MHz part of the proton RF system was responsible for this effect. The reason for this suspicion was the disappearance of the oscillations at energies of 70 GeV. At this energy, the 208 MHz system starts to take over the provision of the buckets from the 52 MHz system. This transition is completed at 150 GeV. But even at the start of this process, the bucket potential becomes more non-parabolic and thus increases Landau damping which damps oscillations. In the case of a malfunction in the 208 MHz system, we expect to observe such oscillations also at higher energies, when the buckets are mainly provided by the 208 MHz RF system.

Surprisingly, all standard parameters from the proton RF controls showed normal values and the storage rings operation was not further interfered. Measurements with respect to RF

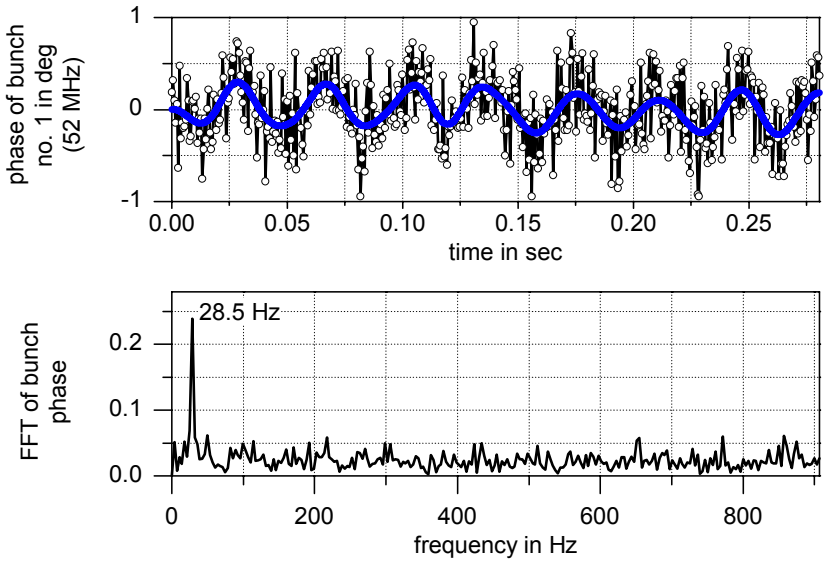

Figure 3.7: Beam phase oscillation of bunch no. 1 and its frequency spectrum at injection energies, observable up to energies of about 70 GeV (March 2003 08:56:28 AM).

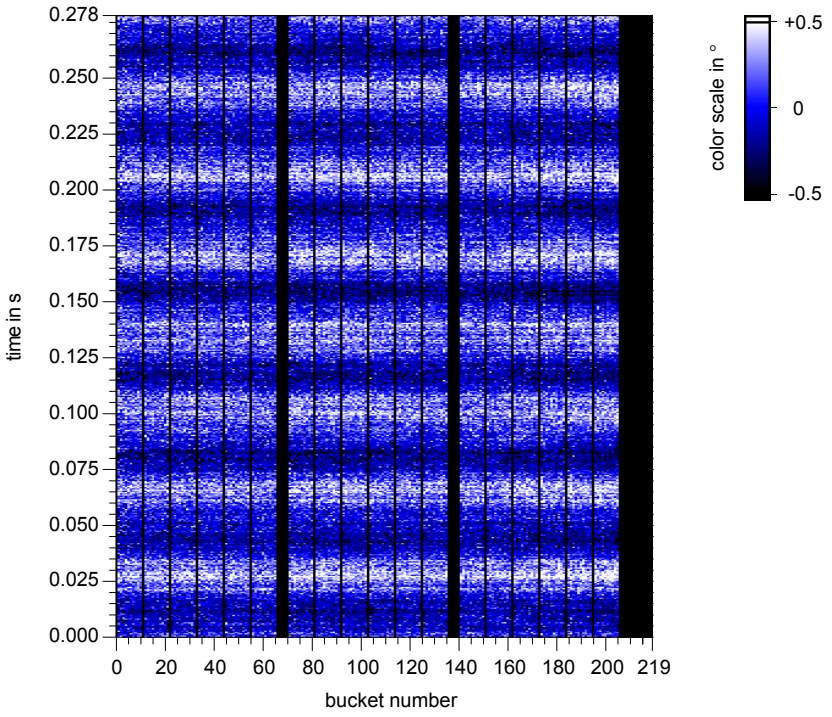

Figure 3.8: Beam phase oscillations. The data was taken on 2. March 2003 at 08:56:28 AM with a beam current of 21 mA.

noise effects, causing coasting beam during long storage times at high energy, performed by S. Ivanov and O. Lebedev[1] [8, 9], showed that the RF in the second 52 MHz cavity was modulated at high energy with about 27 Hz to 30 Hz. They found that this modulation was not equally observable at all other cavities, it was furthermore observable without and with beam. The observed coherent oscillations at low energy may also be driven by this modulation. Indeed, following this hint, one can discover a modulation between 27 Hz to 30 Hz in the data records

[1] both from Institute for High Energy Physics (IHEP) Protvino, Moscow Region, 142281, Russia

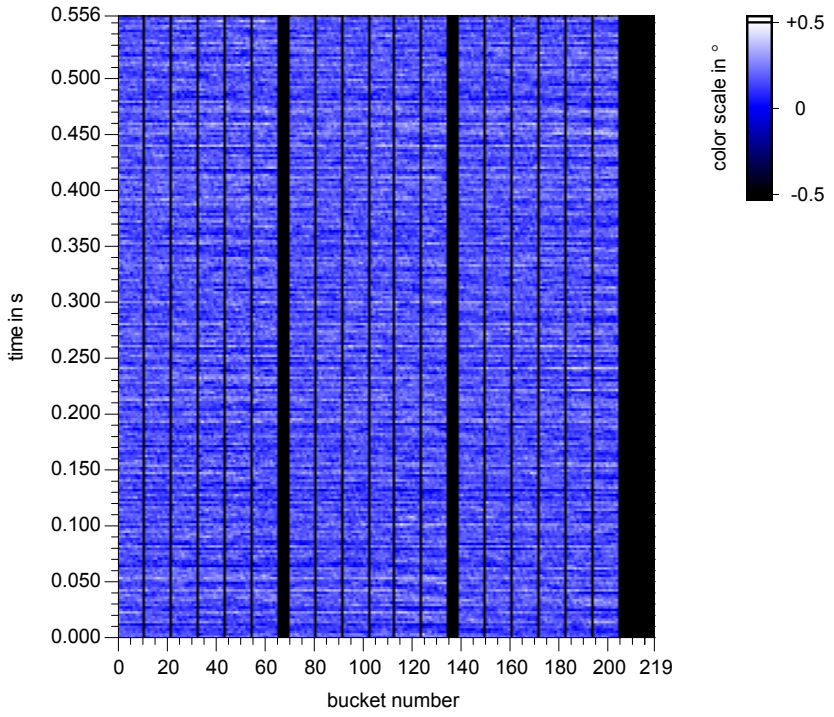

Figure 3.9: There were no obvious strong beam oscillations at injection energies during the HERA operation in 2000. The data shown was taken on 26. July 2000 at 11:12:20 AM with a beam current of 90 mA.

of the FLD taken at low energy. It is visible with high amplitude in the second 52 MHz cavity.

By means of figures 3.10 to 3.13, we will discuss this observation: The figures show the steady state at low energy between the beam induced voltage and its suppression by the RF fast feedback loops in the case of 10 bunches. Each bunch contained $8 \cdot 10^{10}$ particles. In figures 3.10 and 3.11 the RF voltage changes during one turn are plotted. At the bucket positions 1

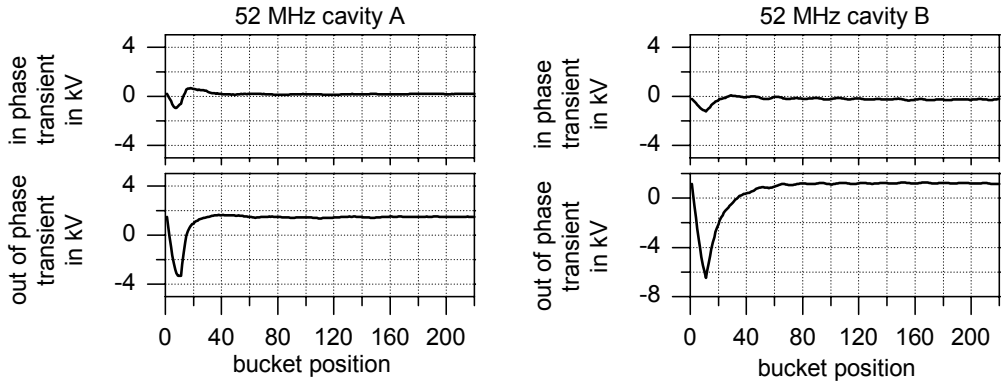

Figure 3.10: Steady state of the voltages in the 52 MHz cavities induced by ten bunches and their suppression by the RF fast feedback loops. The data was taken on 24. February 2003 06:12:30 AM at low energy.

to 10 the bunches induce voltage, resulting in an nearly linear voltage change. After that time, the RF fast feedback loops compensate the induced voltage, following an exponential behavior. The fact that the voltages are not corrected within the same time are evidence that the gains of

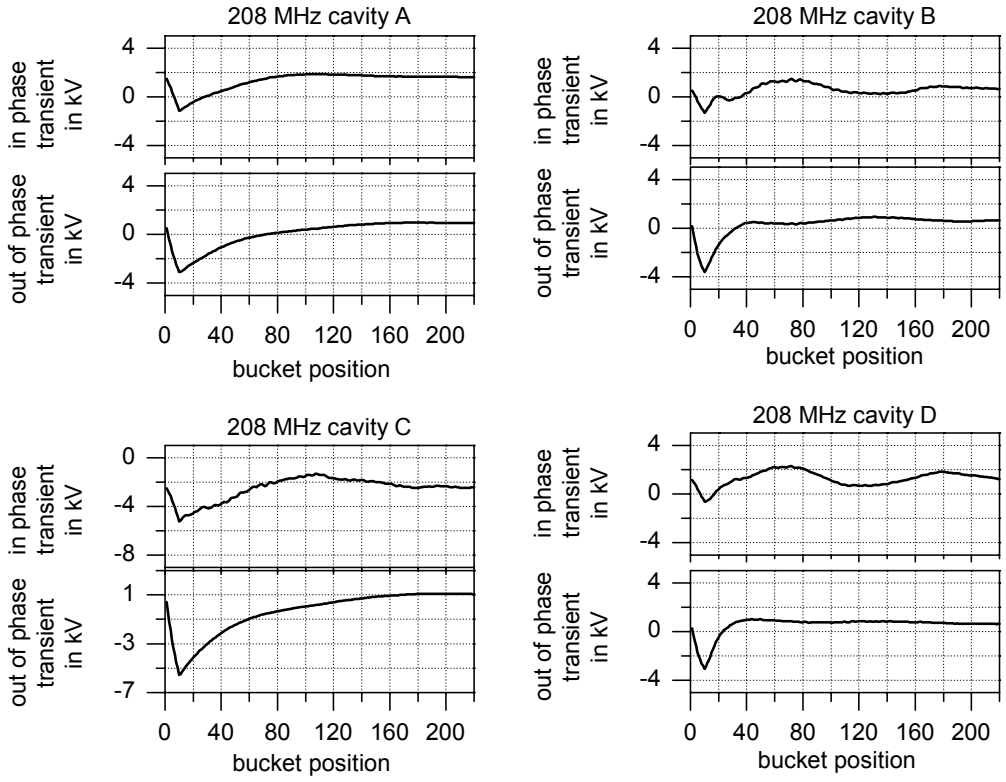

Figure 3.11: Steady state of the voltages in the 208 MHz cavities induced by ten bunches and their suppression by the RF fast feedback loops (24. February 2003 06:12:30 AM).

the fast feedback loops are not equal. For example, the decay time of the 52 MHz cavity B is twice as large as compared to that of the 52 MHz cavity A. Ideally, the second cavity should behave like the first one.

We can examine the behavior of this fast feedback loops in more detail by analyzing the RF voltage change at the bucket position 20. This corresponds to the RF voltage changes seen by a bunch at position 20. In our case there is no bunch, so we observe the behavior of the fast feedback loops themselves. Figure 3.12 shows the frequency spectrum of the voltage changes

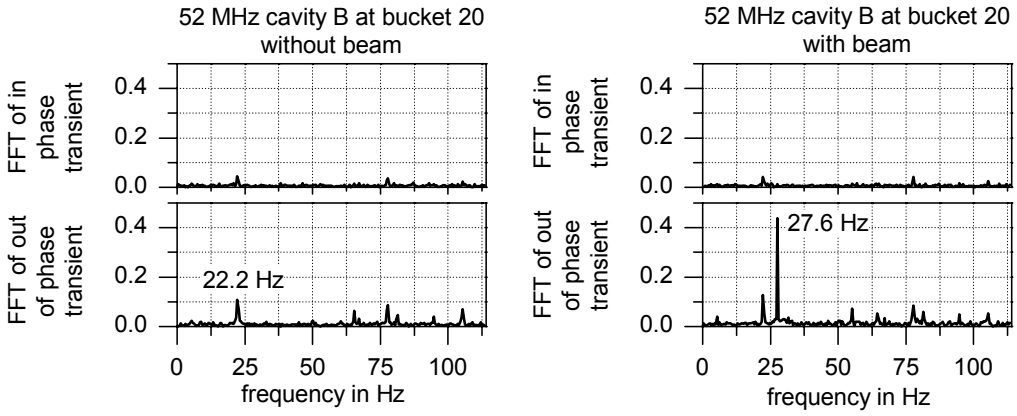

Figure 3.12: FFT of the voltage change at bucket position 20 in the second 52 MHz cavity, without and with 10 bunches at position 1 to 10.

in the 52 MHz cavity B first without and with beam. With beam a remarkable line at 27.6 Hz appears. All other cavities do not show this line or only with much lower strength, see figure 3.13.

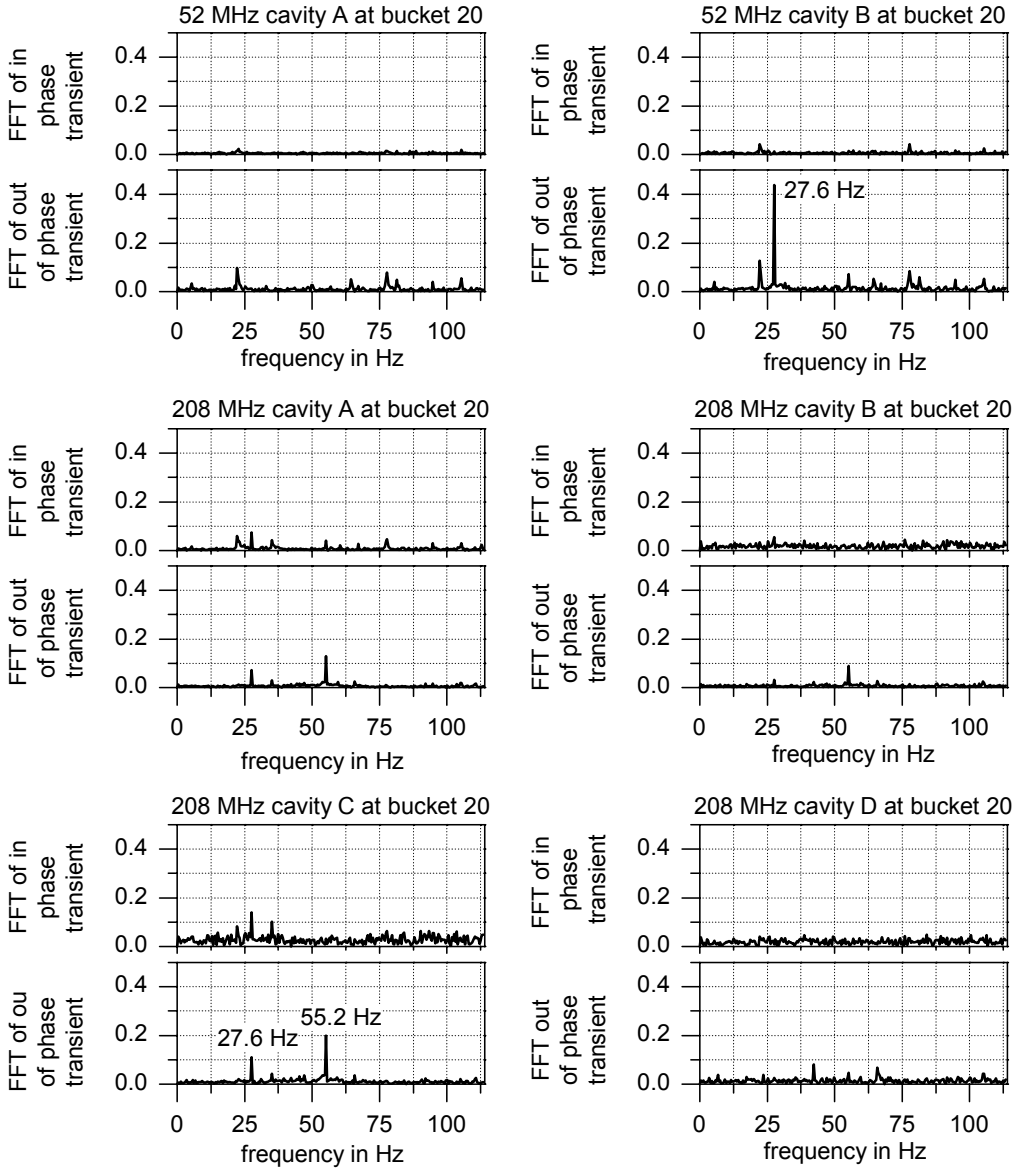

Figure 3.13: FFT of the voltage changes at bucket position 20 in all RF cavities, with 10 bunches at position 1 to 10.

3.3 Coupled Bunch Oscillations above 70 GeV

The strongest longitudinal emittance blow up occurs during the acceleration process above 70 GeV and at high energy, due to coupled bunch oscillations, as reported in [10]. Figure 3.14 shows the development of the longitudinal emittance during acceleration derived from an analysis of recent FLD data. The origin of the time scale corresponds to the start of the acceleration.

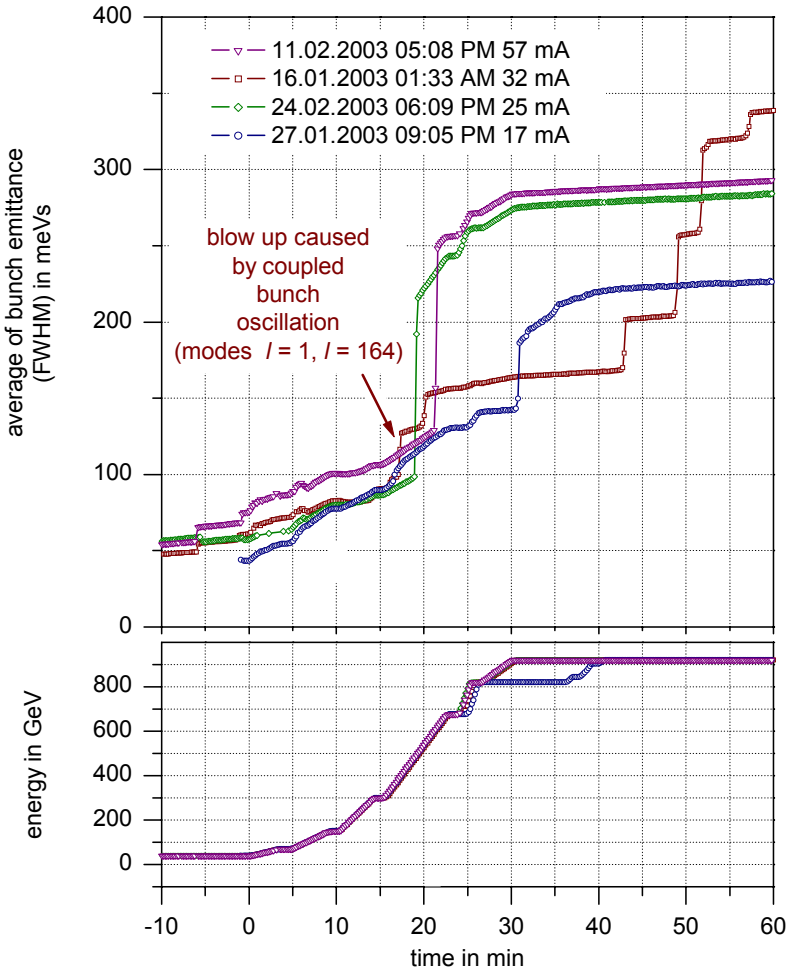

Figure 3.14: Development of the longitudinal proton emittance in HERA during acceleration of 180 bunches from 40 GeV to 920 GeV. The sudden steps are caused by coupled bunch oscillations.

At this time, the initial longitudinal FWHM emittance is about 45 meVs to 70 meVs. Due to the injection of the second and third bunch train, the average emittance changes are caused by beam loading, see section 3.1, and the new injected bunches are also considered in the emittance mean value after an injection. This explains the appearance of the partly observable emittance reduction at injection in figure 3.14.

At the ramps shown, the emittance grows smoothly up to energies around 300 GeV. Above 300 GeV the emittance is blown up in several vast steps. The analysis of the FLD data shows that these steps are caused by coupled bunch oscillations. Figure 3.15 shows for example the coupled bunch oscillation responsible for the marked step in figure 3.14. Even when 920 GeV is reached with a relatively small emittance of 220 meVs, the beam behaves unstably, as the ramp from 16th January indicates.

As an example, consider the coupled bunch oscillation shown in figure 3.15. An interested

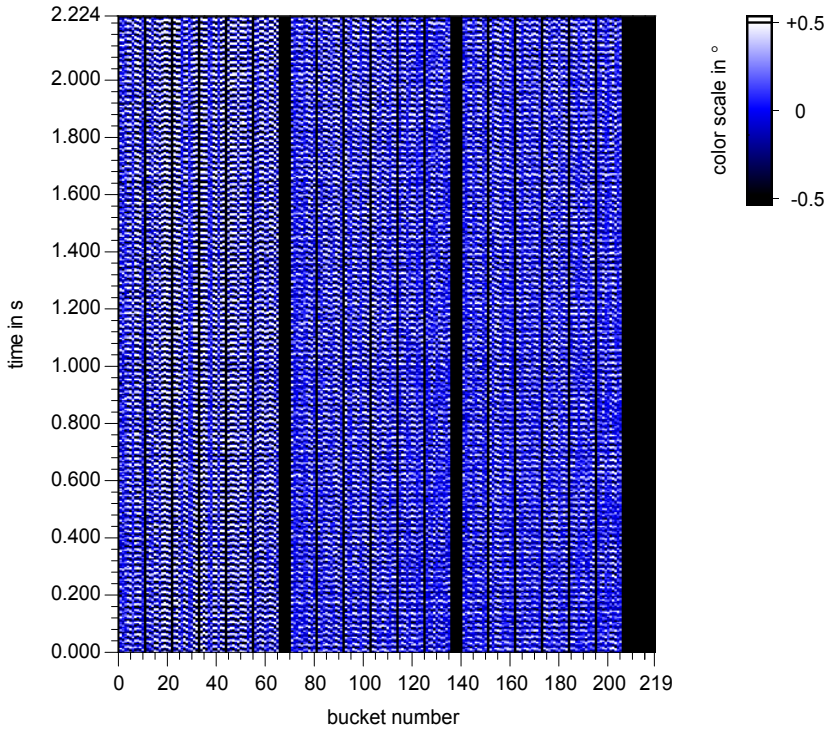

Figure 3.15: This coupled bunch oscillation took place on 16. January 2003 01:50:48 AM at 368 GeV, that was 17 minutes after the ramp started. It increased the longitudinal emittance from 100 meVs to 127 meVs in a sudden step.

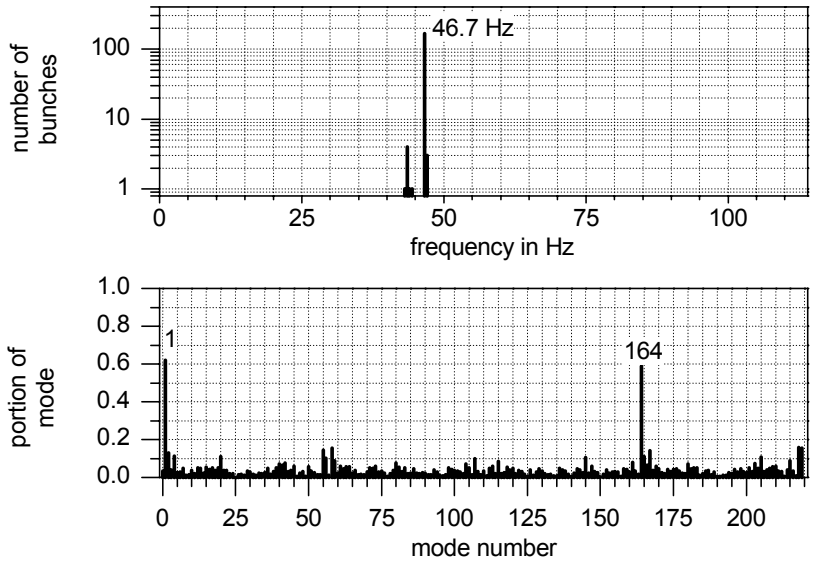

Figure 3.16: Steady state modal analysis of the coupled bunch oscillation of 16. January 2003 01:50:48 AM. The mean frequency is 46.5 Hz and the synchrotron frequency spread 0.6 Hz.

reader, having access to the HERA control system and the FLD, may convince himself that the oscillation shown is typical and one can find much more impressive examples! Figure 3.16 shows the result of the steady state modal analysis of the coupled bunch oscillation. For the underlying principles of this analysis, see [3]. Nearly all bunches are oscillating with the same frequency of 46.7 Hz, as the frequency distribution histogram shows. They are formed in the

modes $l = 1$ and $l = 164$. The oscillation leads to a bunch lengthening within 22 seconds, shown in figure 3.17. After the bunches got longer, they are stabilized by the larger incoherent

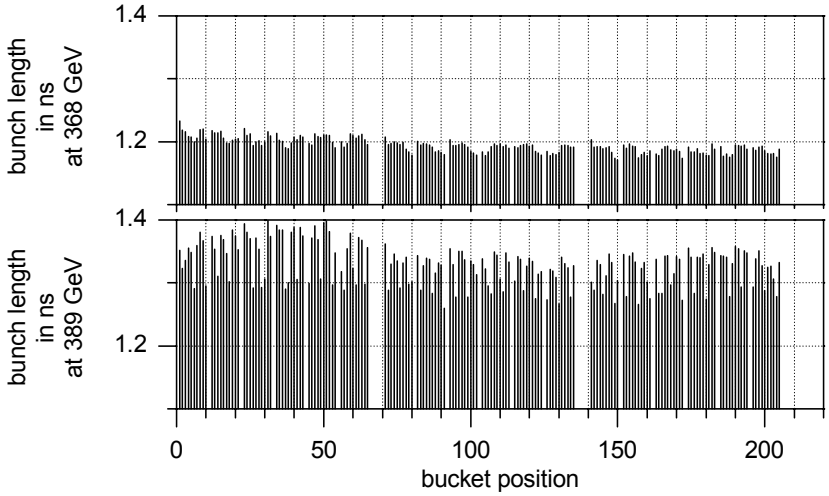

Figure 3.17: Lengthening of the bunches due to the coupled oscillation of 16. January 2003 01:50:48 AM. The upper graph shows the bunch lengths at 01:50:48 AM and the lower 22 seconds later, at 01:51:33 AM. Aside, the shown bunch lengths are recalibrated with CMFL-data.

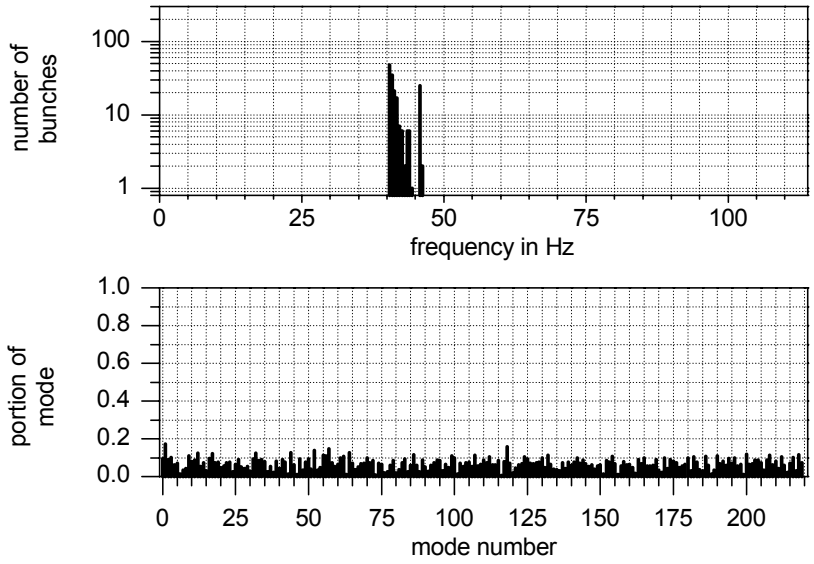

Figure 3.18: Steady state modal analysis of the coupled bunch oscillation of 16. January 2003 01:51:11 AM. The mean frequency is 41.9 Hz and the synchrotron frequency spread is 1.9 Hz.

synchrotron frequency spread and also by oscillating with different frequencies, see figure 3.18. From the mean frequency change, between the coupled oscillation and the free oscillation, one may estimate the coupling impedance. The frequency spread of 1.9 Hz which is obviously able to suppress the coupling, may also be taken to estimate the impedance. Such estimates are already discussed in [3]. But, for the situation presented we have also to consider the synchrotron frequency change due to the changing RF voltages and particle energy during the

acceleration. This change may seriously influence the results, especially when we estimate the coupling impedance from the change of the mean frequency. A more proper way is to examine coupled bunch oscillations taking place after high energy is reached, where the synchrotron frequency of non coupled bunches is no longer changing. Nevertheless, such considerations give rise to the assumption that the longitudinal impedance budget got worse as compared to the situation in HERA I. The problems discussed in section 3.2 in the RF system may be responsible for this behavior.

3.4 RF Noise Effects

Preservation of the longitudinal emittance during acceleration will result in shorter proton bunches at the begin of a luminosity run. To keep the bunches short we have also to suppress longitudinal emittance diluting effects taking place during long beam storage times. Such effects are expected to be also responsible for protons kicked out of the bucket potential forming coasting beam.

The most obvious candidate, RF noise, was examined by S. Ivanov and O. Lebedev[2] [8, 9], as already mentioned. They measured the RF noise spectra by modifying the RF signal paths of the cavity voltage measurements of the FLD, by substituting RF filters and amplifiers. The noise spectra taken from the 208 MHz cavities show somewhat lower noise levels than expected. In contrast, the levels in the 52 MHz cavities are noticeable higher. Discrete frequency lines overlay the continuous noise spectra. In the spectrum of the second 52 MHz cavity a strong line at about 30 Hz is present, which is not visible with the same strength in the other cavities. In their measurements, this line is visible both with and without beam. As the synchrotron frequency at high energy is close to 35 Hz, this line is expected to have a significant influence on the long term development of the longitudinal emittance and the production of coasting beam.

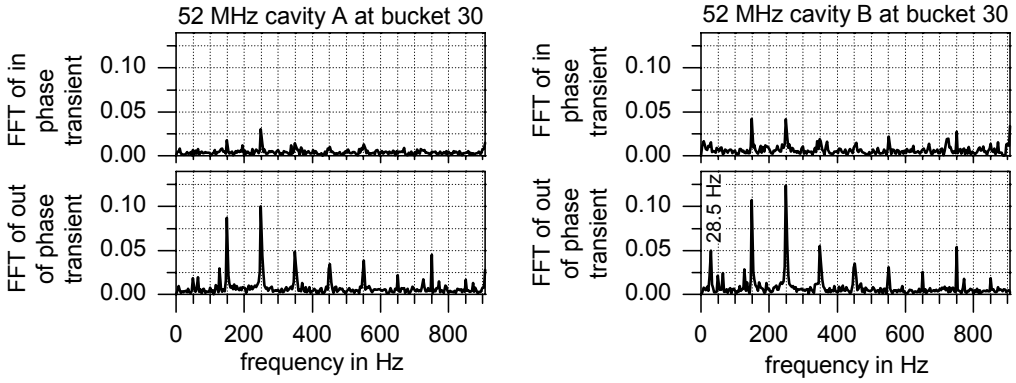

Figure 3.19: FFT of the voltage changes in the 52 MHz cavities. The data record was taken on 1. March 2003 07:31:28 AM with 21 mA beam in 180 bunches at 920 GeV. In the second 52 MHz cavity a line at 28.5 Hz is visible.

The way in which the FLD takes the cavity voltage data is in no way adjusted for RF noise measurements as compared to the method from S. Ivanov and O. Lebedev. Nevertheless, by examining the records taken, one discovers at high energy also a frequency line at 28.5 Hz in

[2]both from Institute for High Energy Physics (IHEP) Protvino, Moscow Region, 142281, Russia

the spectrum of the second 52 MHz cavity, see figure 3.19, which is not observable in the other cavities, figures 3.19 and 3.20.

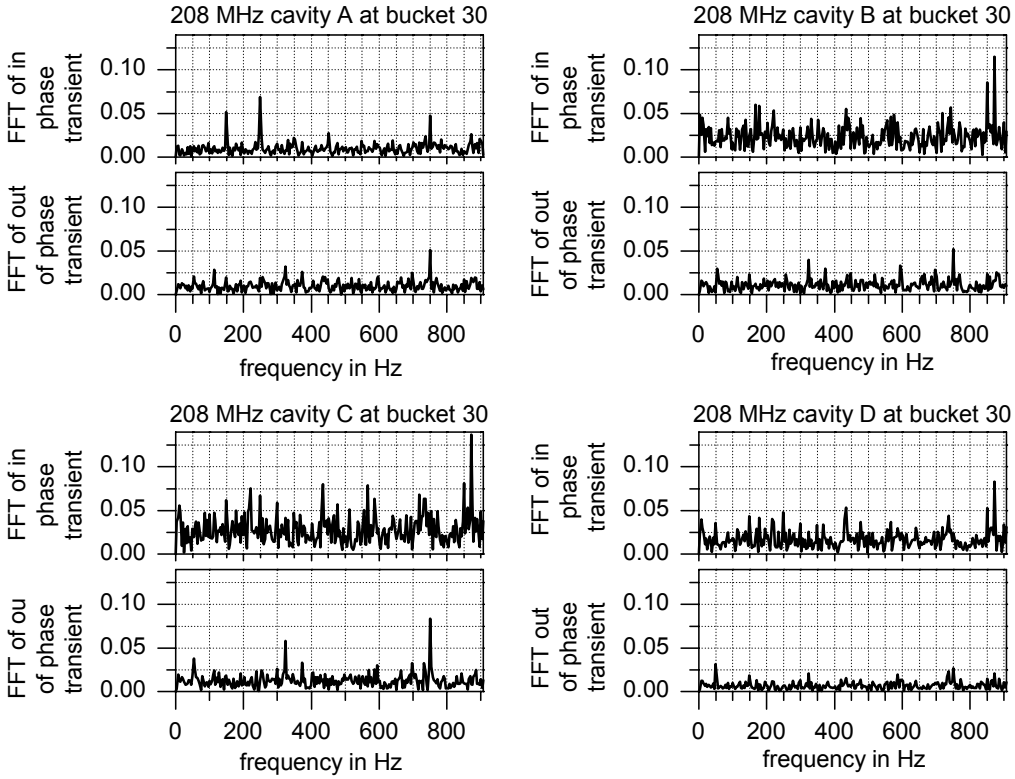

Figure 3.20: FFT of the voltage changes in the 52 MHz cavities. The data record was taken on 1. March 2003 07:31:28 AM. There are no frequency lines visible near the synchrotron frequency of 20 Hz to 40 Hz.

In addition, the strong lines at 150 Hz, 250 Hz may be caused by the mains frequency. A more detailed examination has to verify to what extent they are artificial, that means, caused in the diagnostics system itself. The absence of the lines in most of the 208 MHz systems may be a hint, that these lines are real RF modulations of the cavity voltages.

4 Tested Measures for Emittance Preservation

Beam oscillations, leading to an emittance dilution, may be suppressed by active or passive methods. Active methods are control loops detecting the beam oscillations. Dependent on the detected values, they steer devices acting back on the beam. Typical examples are narrow band feedbacks, like the so called 'Phase Loop II' at HERA, broad band feedbacks, this means coupled bunch feedbacks or a mixtures of both, like the 'Phase Loop I'. In contrast, passive methods increase the intrinsic damping of the beam without considering whether the beam is oscillating or not. For example, Landau damping cavities increase the incoherent synchrotron frequency spread and with that the beam stability. One may also increase the coherent frequency spread. This can be done by $h+1$ harmonic cavities or even an amplitude modulation (AM) of the RF voltage. With both methods, each bunch gets its one bucket potential strength and with that its own synchrotron frequency.

In this chapter, some of these measures, applied to the HERA proton ring and the experience we made, will be discussed.

4.1 The Use of the Phase Loops

At the HERA proton ring, two phase loops with different bandwidth and different control theoretical principles are installed.

The 'Phase Loop I' realizes a differential controller and works as follows: The circulating beam is divided in 22 parts without particular consideration of the actual fill pattern. For each of these 22 parts, the beam phase is measured and fed back as a phase change of the 52 MHz steering signal with a programmable but fixed time delay. This time delay has to be near 1/4 of a synchrotron oscillation cycle. Ideally, this delay time is changed from outside during acceleration following the change of the synchrotron frequency. Until now, this has not been the case at HERA. The loop should damp the coupled bunch modes $l \leq 22$.

Using the default settings of the Phase Loop I, we found with the FLD that this loop is only able to damp beam phase oscillations down to amplitudes of about 2° (52 MHz). Beam oscillations with amplitudes smaller than 2° are not influenced. This may be an indication that the sensor part of this loop is not very sensitive. Unfortunately, technical problems with the remote control of the loop parameters prevented a more careful examination. In the actual situation, the loop is unsuitable for our purpose, because beam oscillations with amplitudes smaller than 2° already lead to a large emittance dilution.

The 'Phase Loop II' realizes an integral controller in the following way: The beam phase is measured with a sensitive narrow band phase detector. Beam phase deviations are transferred to changes of the RF frequency. These frequency changes result in the course of time in phase changes, acting back on the beam. One can show that such a loop is inherently stable. Hence, very large feed back gains are possible. For more details within this respect, see [3]. But, the loop is only able to damp the coupled bunch mode $l = 0$.

In the last HERA run period, the Phase Loop II became the focus of our attention, since the longitudinal proton emittance suffered from beam phase oscillations at low energy in the mode

$l = 0$, as discussed in section 3.2. The loop is an ideal device to suppress these oscillations, as long we localize and eliminate the source driving them. For this purpose, the Phase Loop II should work without restrictions at low energy and during acceleration. Unfortunately, our first attempts to use the loop during acceleration in September 2002, resulted in a confusion in the timing between revolution triggers, bunch clock signals and the beam. In some cases, this was accompanied by high losses of beam intensity. Figure 4.1 shows such an effect, where the

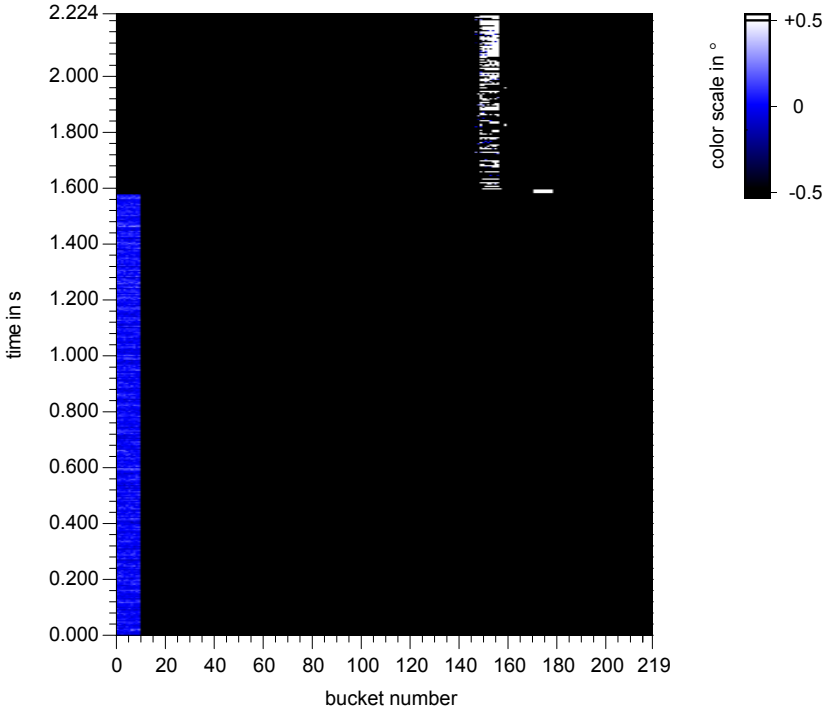

Figure 4.1: A working Phase Loop II during acceleration caused until autumn 2002 sudden shifts between timing signals and the beam. Here, the jump of the FLD revolution trigger resulted in a FLD record showing a 'jumped beam'. The record was taken on 9. September 2002 at 60 GeV with a beam current of about 5 mA.

revolution trigger, generated from the FLD timing, suffers a shift of about 150 bucket positions, resulting in a FLD record showing a jumped beam.

Looking at such pictures, it must be clear, that the beam itself is not able to jump around the storage ring. Therefore, they indicate a jumped timing. Not only the FLD timing jumped. The revolution triggers of the HERA integrated timing (HIT) system jumped too.

Since the loop consists of the phase detection of the beam, the whole HERA frequency generation, some RF phase locked loops and the controls for cavities, we had to take into account all the technical details of these devices for localizing the bug. For an overview on the phase loop and the timing systems, see figure 4.2.

I will not bother the reader with all the discussions and measurements we performed. At the end, Wilhelm Kriens, Uwe Hurdelbrink and Kai Brede from the group MSK found that the data input at the frequency synthesizer had problems with lowering BCD values. This caused jumps in the HERA RF. These jumps were fast compared to a normal synchrotron oscillation cycle, so that the bunches were recaptured in RF buckets after the jumps and in most cases still stored. Since the HIT and the FLD timing uses the RF as source to generate their signals, they also jumped. During acceleration without Phase Loop II, the frequency values increased monotonously and no problems arose. As the phase loop also reduces the frequency for short times, to damp beam oscillations, the bug occurred.

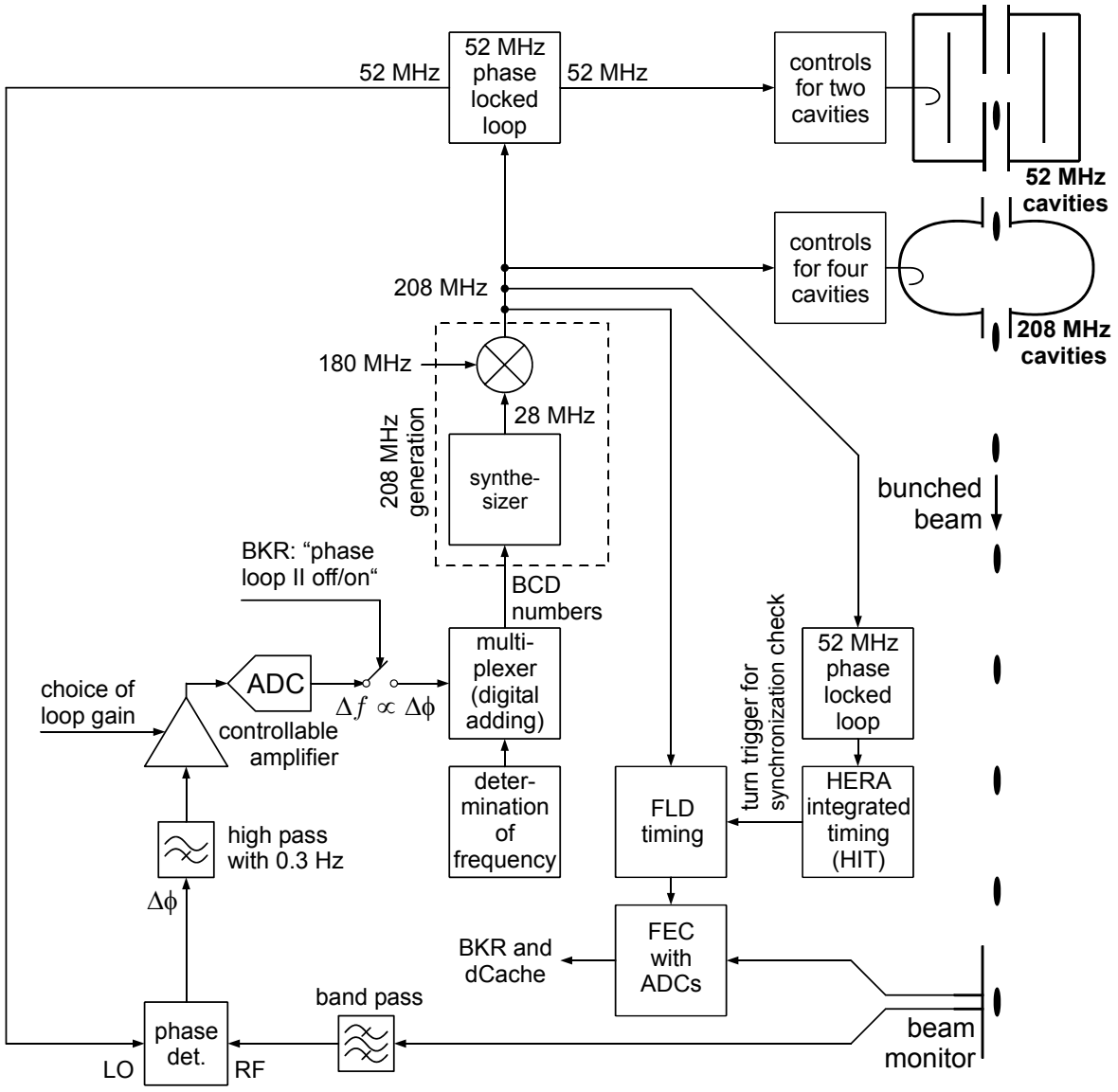

Figure 4.2: The Phase Loop II consists of a narrow band phase detection, whose output is transferred into a change of the frequency values at the RF synthesizer input. The generated 208 MHz RF frequency supplies the cavities controls with RF input signals, partly over a RF phase locked loop. Finally, the loop is closed over the beam. The timing systems use the 208 MHz RF frequency to generate their clock and trigger signals.

Since the bug was fixed in autumn 2002, the loop works to our full satisfaction at low energy, during ramping and at high energy. Figure 4.3 contains an example for a beam oscillation at low energy and its suppression after switching the loop on.

The loop does not only damp beam oscillations of coupled bunch mode $l = 0$, it has also a positive effect on the longitudinal emittance, as figure 4.4 shows for low energy and high beam intensities. Without phase loop, the emittance increase in the case shown with about 1.7 meVs/min, the loop reduces this value to about 0.9 meVs/min. This is a reduction of the growth rate of almost 1/2. At lower beam intensities the improvement achieved by the use of the loop was lower.

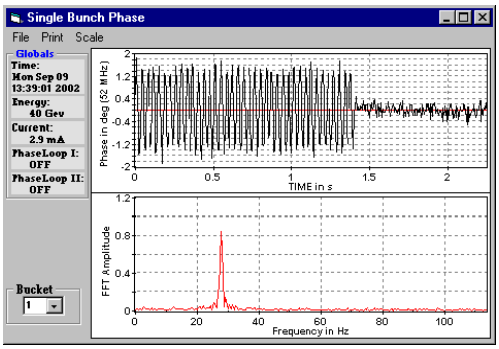

Figure 4.3: Action of switching on Phase Loop II. A bunch phase oscillation with an amplitude of about 1.6° is immediately suppressed.

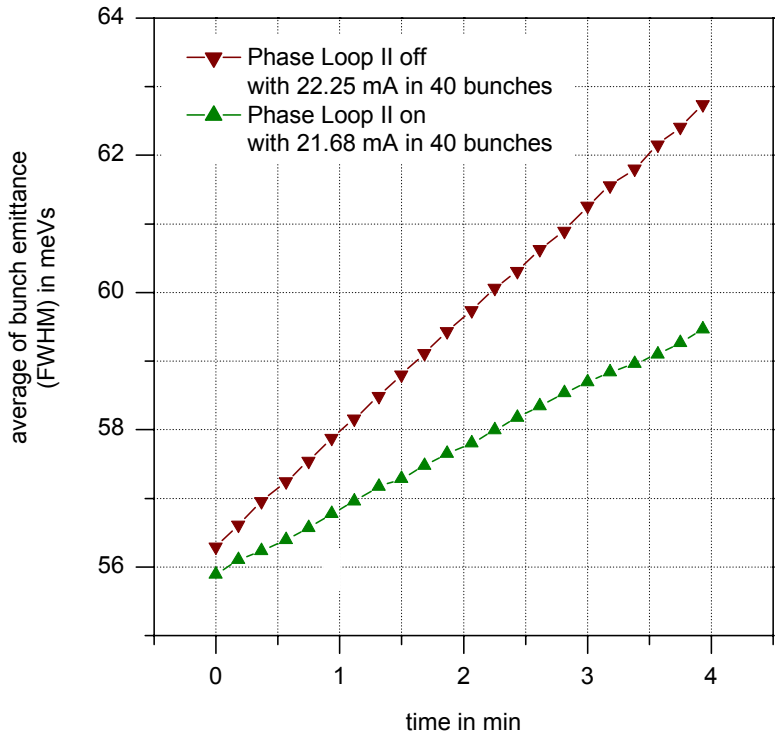

Figure 4.4: Growth of the longitudinal emittance without and with Phase Loop II at high beam intensities, about $7 \cdot 10^{10}$ particles per bunch. The data shown (23. February 2003 11:57 PM and 24. February 2003 06:24 AM) was taken from 40 bunches in one stored bunch train, while waiting for the injection of the second train.

4.2 RF Setting at Low Energy for Landau Damping

In the normal case, the double harmonic RF system in HERA is operated at low energy so that the higher harmonic (208 MHz) RF system generates no net voltage. Due to the technical properties of the cavity control loops, especially the behavior of the tuner loops in the presence of beam loading, it is not possible to switch the 208 MHz cavities on during acceleration. Hence, the cavity control loops already require control signals before the beam is stored. To

achieve zero voltage at injection, three 208 MHz cavities operate in phase, whose sum voltage is compensated by the fourth cavity, operating in counter phase.

Normally, at low energy, the bucket potential is only provided by the 52 MHz system. By changing the voltage of 208 MHz cavities we can use them as Landau damping cavities. Hence, we may increase the incoherent frequency spread $s_f = \frac{s_\omega}{2\pi}$. Typically, in a 4th harmonic Landau damping system one uses a voltage for the higher harmonic RF system of about one fourth of the lower harmonic RF system in the bunch shortening mode, that mean, both voltages have the same sign [11, 12].

When $h_{12} = \frac{h_2}{h_1}$ is the ratio of the harmonic numbers and $r_{12} = \frac{V_2}{V_1}$ is the ratio of the RF voltages, the frequency spread can be estimated for $r_{12} < 1 \,/\, h_{12}$ and Gaussian bunches with

$$s_\omega = -\frac{1}{16}\frac{1 + r_{12}\, h_{12}^3}{\sqrt{1 + r_{12}\, h_{12}}}\,\omega_{s0}\;\Delta\phi_\sigma^2. \tag{4.1}$$

In this expression, ω_{s0} is the synchrotron frequency for small oscillation amplitudes and $V_2 = 0$. The half bunch length expressed in RF radians $\Delta\phi_\sigma$ can be obtained from

$$\Delta\phi_\sigma = \frac{l_{FWHM}}{2\,\beta\,c\,\sqrt{\ln 4}}\,2\,\pi\,h_1\,\omega_{rev} \tag{4.2}$$

with the FWHM bunch length l_{FWHM}, the RF frequency $\omega_{RFI} = h_1\,\omega_{rev}$ and $\beta = \frac{v}{c}$. For Gaussian bunches the relation between frequency spread and decoherence times is

$$\tau_d \approx \frac{0.655}{|s_\omega\,|}. \tag{4.3}$$

A derivation of these formulae together with a discussion of their area of applicability is given in [3].

For a bunch length of $l_{FWHM} = 2.4\,\text{ns}$, we get a frequency spread of $|s_f| = 0.21\,\text{Hz}$ and a decoherence time of $500\,\text{ms}$ when the 208 MHz voltage is zero and the synchrotron frequency is $f_{s0} \approx 30\,\text{Hz}$. By increasing the 208 MHz voltage to one fourth of the 52 MHz voltage we increase the spread to $|s_f| = 2.5\,\text{Hz}$ and reduce the decoherence time to $40\,\text{ms}$, leading to an additional damping of beam phase oscillations.

At HERA, a higher 208 MHz sum voltage can be obtained simply by a reduction of the voltage of the fourth cavity operating in counter phase. Figures 4.5 and 4.6 show the reduction of the bunch lengthening caused by injections when one lowers the voltage of the fourth 208 MHz cavity by about 40 kV. The Phase Loop II was used in both cases to damp the coupled bunch mode $l = 0$. Without additional Landau damping, we observed in the case shown a bunch lengthening due to injections of about 40%. With additional Landau damping, introduced by the 208 MHz RF system, we reduced this value to about 5%.

Unfortunately, none of the data records from the injections without additional Lanuau damping, discussed with figure 4.5, show an injection process itself. Figure 3.3 shows also the effect of an injection without additional 208 MHz voltage, but with a higher beam current (69 mA). One observes a weakly damped beam oscillation with relatively long decoherence time $> 250\,\text{ms}$. From the injection with additional Landau damping we have a data record showing directly an injection process. In figure 4.7 the phase, length and intensity of a already stored bunch is shown at the time of the injection of the third train. From the exponential decay of the bunch phase oscillation we obtain a decoherence time of about 40 ms, which agrees with our calculations.

The bunch shown suffered no loss of intensity. This was not the case for all bunches. The data record shows intensity losses mainly at the newly injected bunches and only small losses at

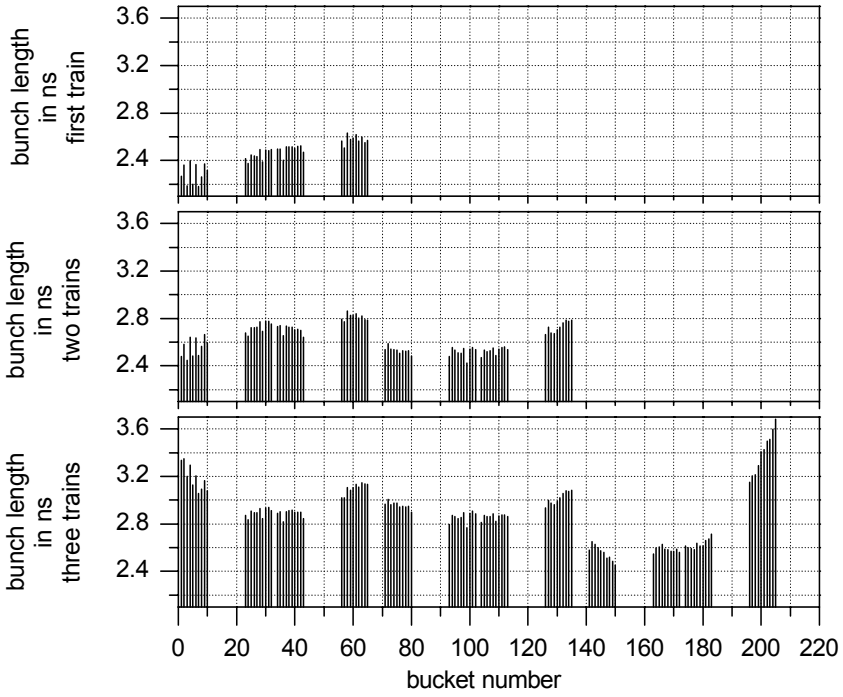

Figure 4.5: Bunch lengthening during injection of three bunch trains with a final beam current of 53 mA (21. February 2003 02:47 PM). The 208 MHz sum voltage was near zero and the Phase Loop II in operation.

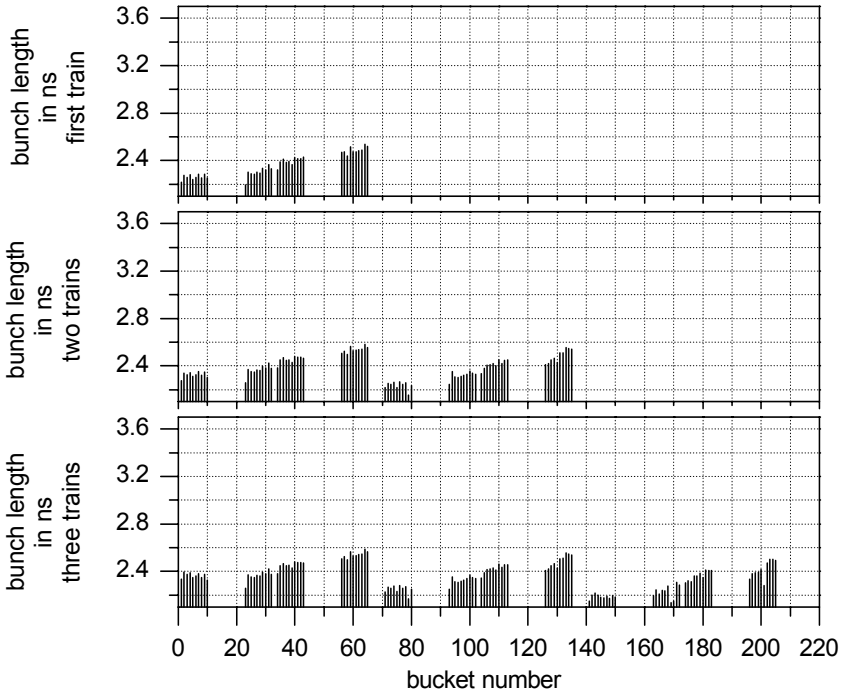

Figure 4.6: Bunch lengthening during injection of three bunch trains with a final beam current of 50 mA (22. February 2003 02:01 PM). The 208 MHz sum voltage was about 40 kV, this is around 1/4 of the 52 MHz voltage of 140 kV. In this case, the Phase Loop II was in operation, too.

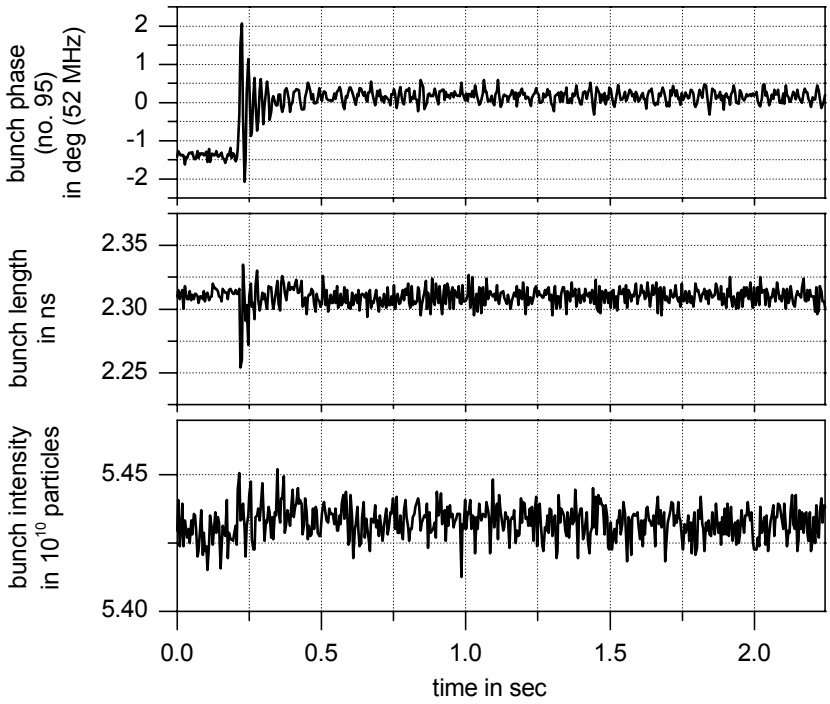

Figure 4.7: Oscillation of the already stored bunch at position 95, increase of its length and the loss of intensity due to the injection of the third bunch train. To damp the beam oscillations, the 208 MHz sum voltage was about 1/4 of the 52 MHz voltage to introduce additional Landau damping.

the first ten bunches. But these effects are small as compared to the situation without additional 208 MHz voltage.

In the HERA run period before the luminosity upgrade, that was in 2000, we measured decoherence times after applying particular RF kicks [3]. At that time, we measure decoherence times more comparable to the value obtained now with additional 208 MHz voltage. In 2000, the 208 MHz sum voltage was also programmed to be zero. To resolve these inconsistencies, we must re-examine the cavity voltage calibration.

4.3 RF Amplitude Modulation

An oscillating bunch leaves oscillating beam loading voltages and wake fields behind, acting on subsequent bunches. Bunches suffering a driving force oscillating with their synchrotron frequency respond with the largest oscillation amplitudes. Hence, bunch oscillations result in a chain reaction when all bunches have similar synchrotron frequencies, resulting in an coupled bunch oscillation, respectively instability. By giving each bunch its individual synchrotron frequency, we can interrupt this chain reaction and suppress coupled bunch instabilities. Variations of the synchrotron frequencies over a bunch train require variations of the RF sum voltage seen by the individual bunches.

4.3.1 Using a $h + 1$ cavity

One method to obtain a variation of the RF sum voltage is to operate some of the cavities in a storage ring with a slightly different harmonic number. For example, we may operate a cavity

with the harmonic number $h+1$. Then the sum voltage will vary from $V_h - V_{h+1}$ to $V_h + V_{h+1}$ over one revolution, but every bunch still sees a constant voltage. This method was already discussed with $h-7$ ($h=84$) cavities in 1988 for the Fermilab Booster [13].

Following the derivation in appendix A.1, we may obtain a bunch to bunch synchrotron frequency spread S_f with a $h+1$ cavity at HERA of

$$\frac{S_f}{f_{s0}} \approx 5\,\frac{V_{h+1}}{V_h}, \tag{4.4}$$

where f_{s0} is the small amplitude synchrotron frequency, V_h the 'normal' RF voltage and V_{h+1} the voltage of a cavity running at a $h+1$ harmonic RF frequency.

According to Sacherer [14], a rule-of- thumb for de-coupling coupled bunch oscillations is that the spread in individual bunch frequencies should exceed the frequency shift $|\Delta f_l|$ due to the coupling:

$$\text{(coherent) spread} \;>\; \text{shift} \tag{4.5}$$

$$S_f \;>\; |\Delta f_l| \qquad \text{for de-coupling.} \tag{4.6}$$

In 3.3 we discussed the measurement of a frequency shift due to the coupling of about 2 Hz. That means, we have to introduce a spread of $S_f > 2\,\text{Hz}$. To guarantee proper working RF controls, the minimum voltages at the HERA RF cavities are 30 kV (V_{h+1}). With a sum voltage V_h at high energy of 540 kV this would result in a spread of $S_f \approx 8\,\text{Hz} > 2\,\text{Hz}$, which should be sufficient for suppressing the observed coupled bunch instabilities.

However, a disadvantage of this method is a systematic variation of the bunch to bunch spacing, lowering the luminosity. For example, a bunch centroid shift of 5° (52 MHz), reduces the luminosity at this collision by about 5% [15], because of the small β-function. For the ratio given above of $\frac{V_{h+1}}{V_h} = \frac{30\,\text{kV}}{520\,\text{kV}}$ we estimate with (A.10) maximum bunch phase deviations of $\pm 3.5°$. The resulting loss of luminosity may be tolerable. But, another problem may be the bucket matching at injection, and ensuring that all bunches have the same bucket potential for Landau damping, as discussed in section 4.2.

4.3.2 Direct RF amplitude modulation

During the last HERA run period, we tested another possibility to increase the bunch to bunch synchrotron frequency spread. We modulated the amplitude of the RF drive signals of cavities themselves, without influencing the phasing. In contrast to a $h+1$ solution, this method requires more RF power. But it has some operational advantages. For example, one can easily switch it on and off during acceleration.

Following the calculations of appendix A.2, the frequency spread introduced by the modulation amplitude of V_{mod} is

$$\frac{S_f}{f_{s0}} \approx 5\,\frac{V_{\text{mod}}}{V_0} \qquad \text{for} \quad \frac{V_{\text{mod}}}{V_0} < 0.6, \tag{4.7}$$

where V_0 is the RF voltage without amplitude modulation. To provide a spread of $S_f > 2\,\text{Hz}$ with $f_{s0} \approx 30\,\text{Hz}$ and $V_0 = 520\,\text{kV}$, we need a minimum modulation amplitude of about $V_{\text{mod}} \approx 7\,\text{kV}$. As we will see, such values are easily obtainable with the HERA proton RF systems.

At injection energy we do not want to modulate that RF amplitude, which is required for correct RF conditions during injections. As the coupled bunch instabilities occur at higher energies, it is possible to delay the modulation until the transition from the 52 MHz buckets to the 208 MHz buckets. This is the case at energies higher than 150 GeV, compare figure 4.8.

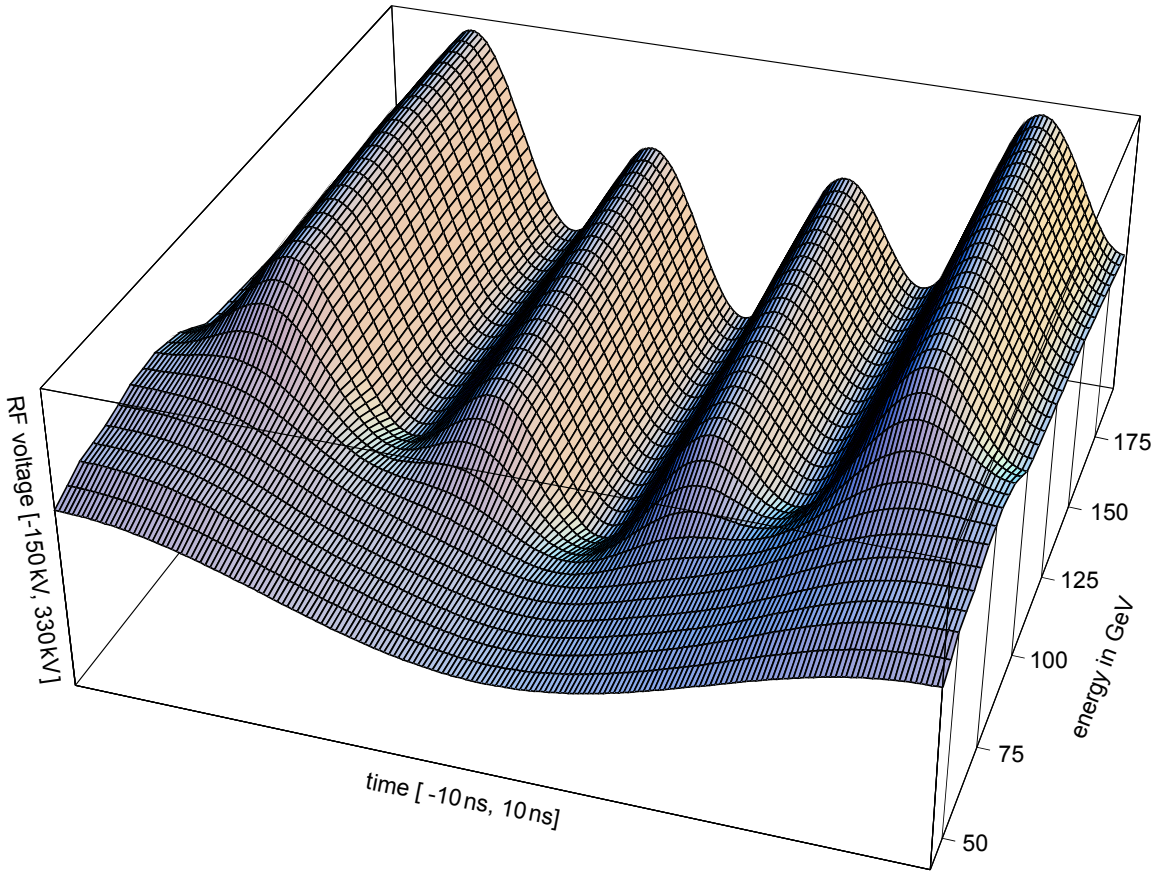

Figure 4.8: Bucket transition during acceleration of protons in HERA, starting from a 52 MHz bucket at injection to a 208 MHz bucket at higher energies. For comparison, typical FWHM bunch lengths at injection are 2.4 ns.

After reaching 150 GeV it is sufficient to modulate only the amplitude of 208 MHz cavities. The test setup used is shown in figure 4.9.

To generate the envelope of the RF amplitude modulation (AM), we use a HP 8112A Pulse Generator which is triggered by a revolution trigger supplied by the FLD timing. We adjusted the generator to produce a triangular output signal in the range between ± 1 V. By supplying this signal to the I input of an IQ modulator, a 208 MHz RF signal is generated and added to the steering signal of a cavity, as shown in figure 4.9. The cable length between the pulse generator and the IQ modulator is experimentally adjusted so that at energies above 150 GeV only the RF amplitude is influenced. As the signal combination is performed within the slow amplitude and phase regulation loop, possible errors in the mean RF values are automatically corrected. For a more detailed description of the RF system itself see [3].

We are able to switch the modulation on and off via the GPIB connection of the pulse generator to a UNIX workstation and to choose the modulation strength from a console in the control room. The workstation and the software are very kindly serviced by Uwe Hurdelbrink from the group MSK.

The first graph in figure 4.10 shows the beam loading in the 208 MHz cavity A at 150 GeV. After switching the AM on, the RF voltage changes, so that a bunch at bucket 80 sees about 80 kV less than one at bucket 205, as shown in the second graph in figure 4.10. With our simple modulation technique, we also influence the phasing somewhat. A more sophisticated

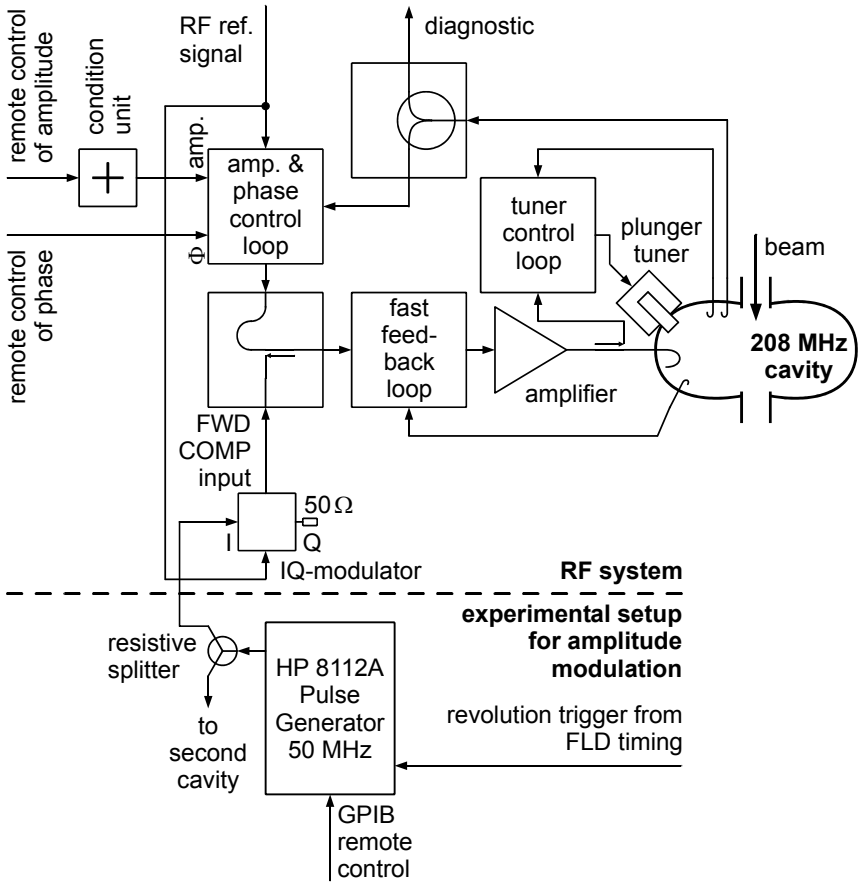

Figure 4.9: Test setup for 208 MHz RF amplitude modulation to suppress coupled bunch oscillations.

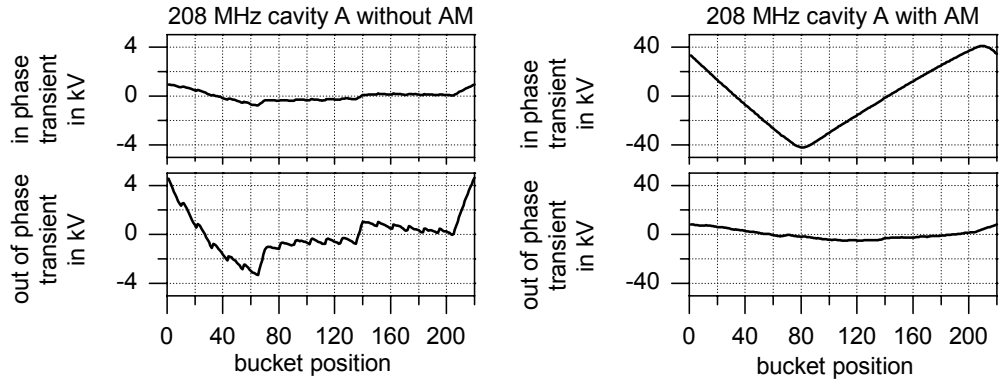

Figure 4.10: Measured beam loading at 150 GeV before and after switching on the amplitude modulation (26. February 2003 06:48 PM).

method may eliminate these phase changes. We will discuss that in the next chapter. But, for the moment we will neglect these small phase changes.

4.3.3 Experiences made with the direct RF amplitude modulation

Before using the amplitude modulation (AM) during a standard proton acceleration, we performed several tests. First, we tested, whether the RF system itself tolerated such modulations without malfunction without beam, followed by tests with stored beam at 920 GeV. Having encountered no problems, we extended our activities to normal proton accelerations during standard HERA operation. In January and February 2003, the AM was in operation during 16 ramps. On seven occasions it was active during the whole proton storage at 920 GeV. With the exception of one instance, it never caused beam losses, in the most unfortunate cases the coupled bunch instabilities were not suppressed and we observed bunch lengths comparable to those after ramps without AM. The event with beam loss was caused by an operating error.

During the first ramps with modulation, we used only one 208 MHz cavity to provide a AM between 30 kV and 40 kV. As we still observed coupled bunch oscillations, we also applied the modulation to a second cavity, to double the amplitude. It turned out, that permanent use of the Phase Loop II together with the AM is necessary, to successfully suppress the instabilities.

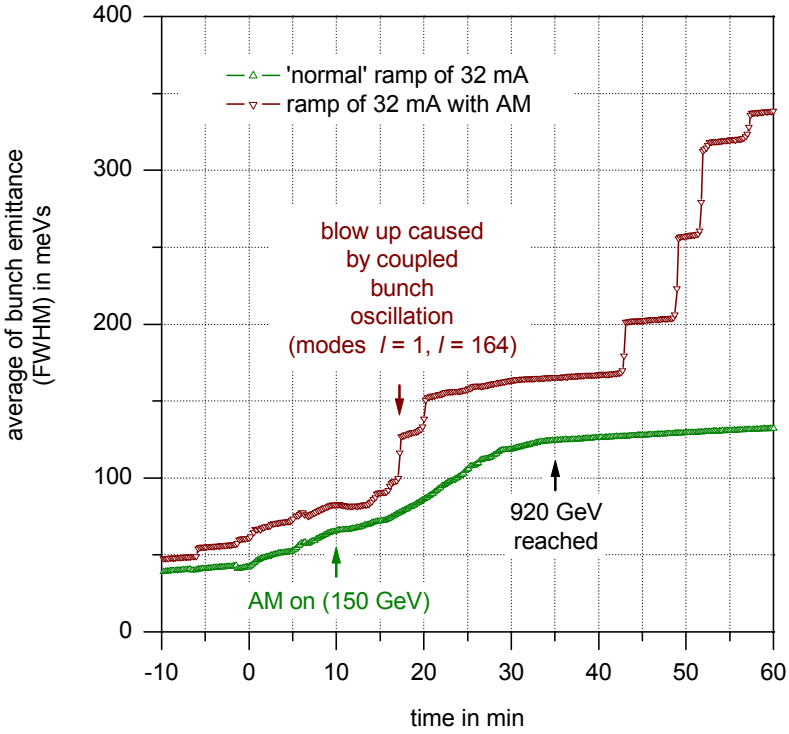

Figure 4.11: Two ramps (both 16. January 2003) with similar beam current, one with and one without amplitude modulation.

Permanent use of the Phase Loop II result in some operational difficulties for the synchronization of the electron ring to the proton ring. As both the synchronization and the phase loop influence the frequency generation, one has to supervise the difference frequency between both rings to be positive during the synchronization process. If the phase loop responds to a beam oscillation such, that this difference frequency would become negative, the synchronization will not lock the correct bucket positions of both rings on each other. Then, the electron bunches would not hit the proton bunches within the experiments H1 and ZEUS. If one detects the possibility of negative difference frequencies, one has to switch the phase loop off during the locking process of the synchronization. Afterwards it has to be immediately switched on. For details on the principles of the synchronization loop and the Phase Loop II, see [3].

To get an impression of the effect achieved by the AM, we will here compare pairs of proton ramps with similar beam current. Figure 4.11 show as first example the development of the longitudinal emittance during ramps performed on 16th January, each with a proton beam current of 32 mA. Without AM, the beam suffered coupled bunch instabilities causing a stepwise blow up of the longitudinal emittance. The RF modulation applied to one 208 MHz cavity, with an amplitude of about 37 kV, generated a bunch to bunch synchrotron frequency spread, suppressing coupled bunch instabilities. Although there were some beam oscillations visible during the ramp with AM, the emittance was more than a factor of two smaller as compared to the value reached without modulation.

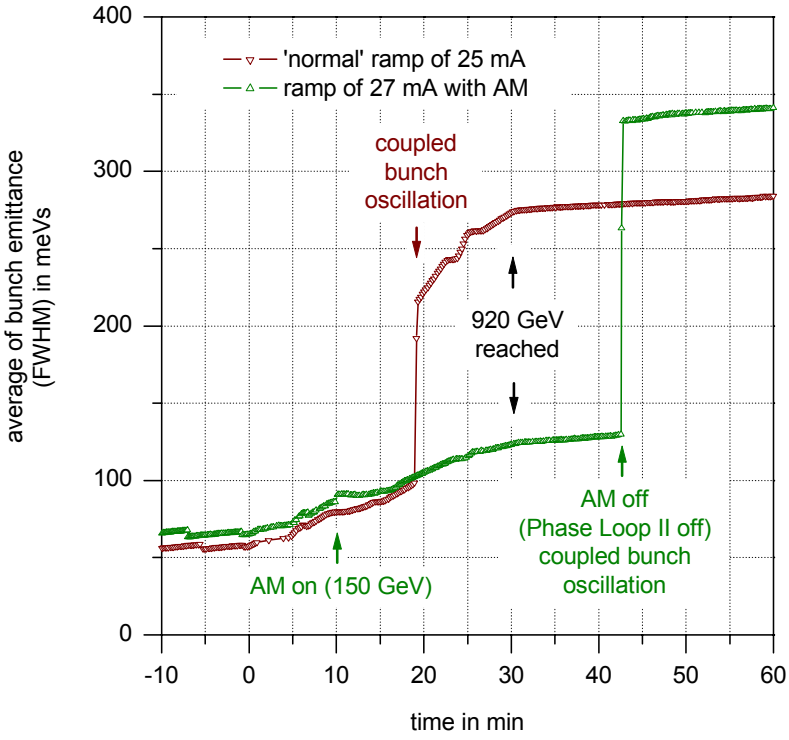

Figure 4.12: Two ramps (24. and 26. February) with nearly similar beam current of about 26 mA. To perform a cross check of the action of the modulation and phase loop, we switched both off, 12 minutes after reaching problem-free 920 GeV.

The efficacy of the AM can also be checked in the following way: We accelerate protons with the amplitude modulation, to suppress the instabilities and get short bunches at high energy. We ensure that the beam is stable, by waiting with active AM and phase loop for some time after reaching 920 GeV. For example we wait 10 minutes. Then, we switch off both, the AM and the phase loop and observe, whether coupled bunch oscillations arise, causing an emittance blow up. Figure 4.12 shows the result of an test of this idea. In contrast to the ramp shown in figure 4.11, we applied the modulation onto two 208 MHz cavities, resulting in an modulation amplitude of 78 kV. During this ramp (AM on), no strong beam oscillation was visible. In this case, we got also a reduction of the longitudinal emittance of an factor of two due to the AM. The corresponding bunch lengths are about 0.97 ns. After switching the AM and the phase loop off, a strong coupled bunch oscillation occurred resulting in a considerable emittance blow up. The bunch length increased to typical values of about 2 ns. For completeness, figure 4.13 shows the beam oscillation which arose.

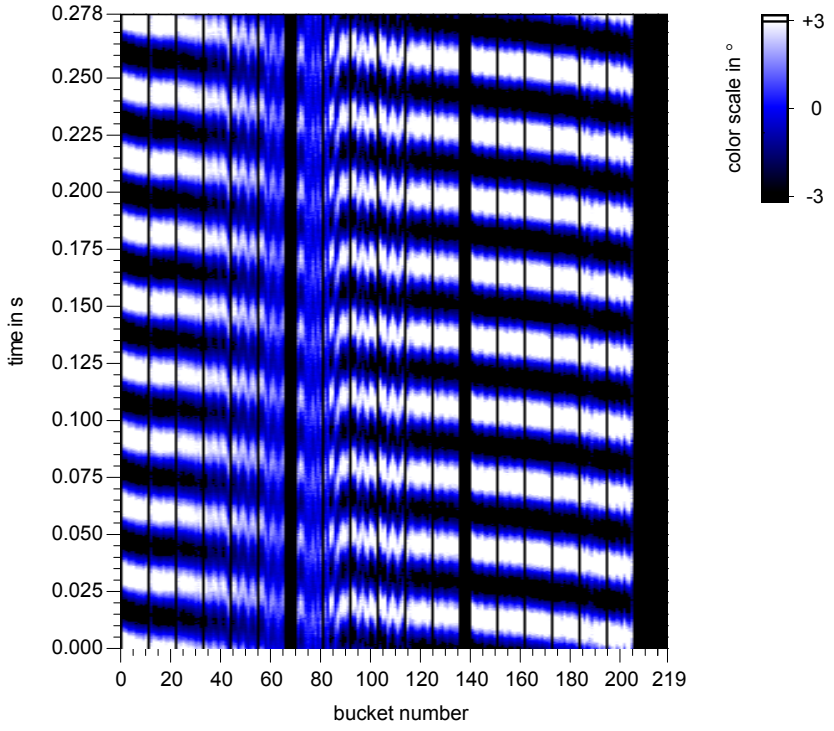

Figure 4.13: This coupled bunch oscillation occurred after switching the AM and the phase loop off at 920 GeV and initial bunch lengths of 0.97 ns (26. February 2003 07:21:04 PM).

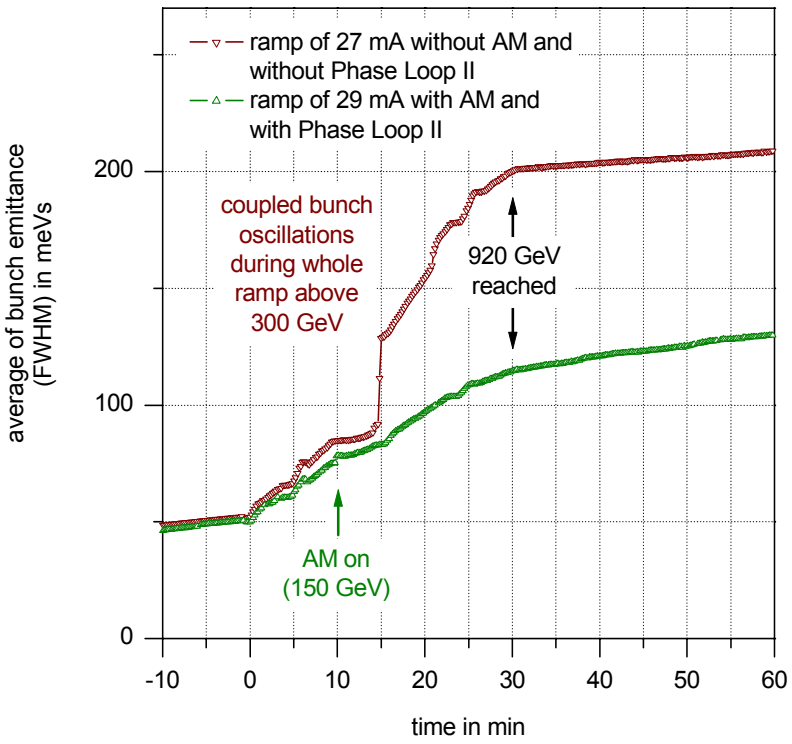

Figure 4.14: Again two ramps (08. and 10. February) with nearly similar beam current of about 28 mA. After both ramps the protons was successfully brought into collision with electrons.

The final goal of the activities presented here, is to make luminosity with short bunches. Therefore, we had to show that this is possible in practice without problems. Figure 4.14 shows again two ramps with comparable beam current. By permanently using the Phase Loop II and switching the AM on at 150 GeV, we obtained a longitudinal emittance at 920 GeV which was nearly a factor of two smaller, as compared to a ramp without phase loop and without AM. After both ramps the proton beams was successfully brought into collision with electron beams, resulting in nearly the same specific luminosity of about 2 $\frac{10^{30}}{\mathrm{cm^2\ s\ mA^2}}$, measured at H1. This is slightly over the design value of 1.8 $\frac{10^{30}}{\mathrm{cm^2\ s\ mA^2}}$.

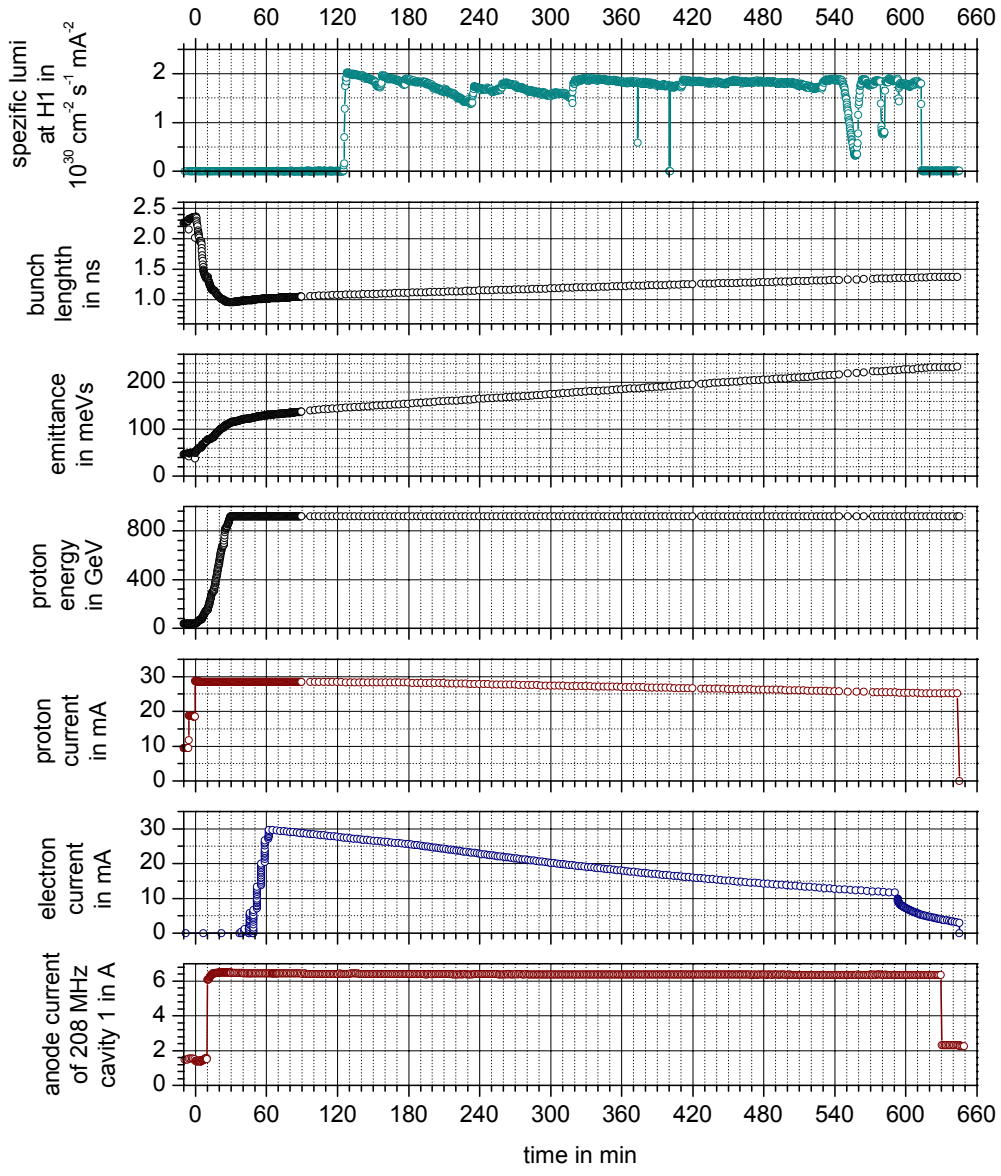

Figure 4.15: Luminosity run on 10. February with Phase Loop II permanently in operation and AM in operation from 10 min to 630 min.

Figure 4.15 shows the longitudinal beam behavior during the luminosity run with AM and phase loop in operation. For orientation, the AM was switched on 10 min after the proton ramp start, which is the origin of time scale in figure 4.15. It was then in operation for 620 min. After

reaching 920 GeV, one still observes an increasing emittance over several hours. But, the key point is, that the longitudinal proton emittance shows a value of 230 meVs at the end of the run. 'Normal' luminosity runs shows at the begin values larger than 230 meVs.

For an examination of the luminosity gain, achieved with the shorter bunches, future studies have to take into account the transverse beam dimensions by measuring them with wire scanners. Unfortunately, this was not done during the luminosity run presented here.

The time constant of a 208 MHz cavity in HERA is 41 μs [3], that is twice the HERA revolution time of 21 μs. The time period of the AM is equal to the revolution time. This means, that the RF modulation of 47 kHz is damped by the cavity itself due to its bandwidth of 24 kHz. Nevertheless, we are able to produce maximum modulation amplitudes at a 208 MHz cavity between 30 kV and 40 kV. This is achieved by a more than three times higher power drain on the RF amplifiers as compared to the normal case. One can observe this fact at the anode currents of the final stage RF amplifiers. At the 208 MHz systems from HERA, they show typical values of 1.8 A without AM, with AM they are increased to 3.3 A. The fact that we are not able to increase the modulation amplitudes to values larger than 40 kV is explained by power limits of the final stage amplifiers. In figure 4.15, the last graph shows the anode current of the first 208 MHz cavity during the luminosity run with AM.

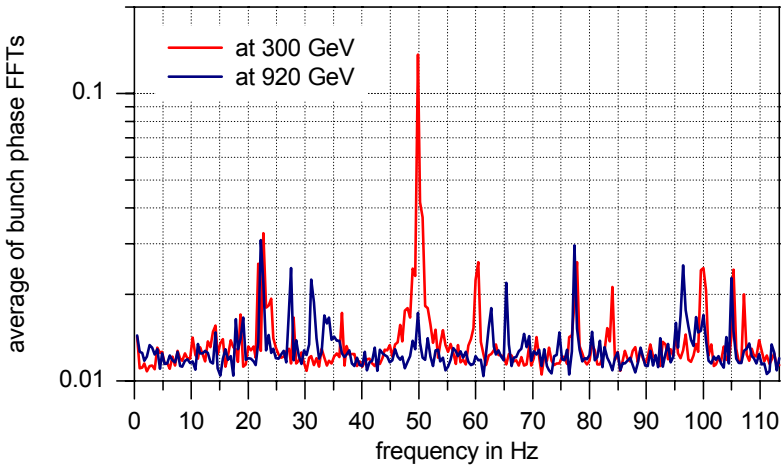

Figure 4.16: By summing up the FFTs of all bunch phase oscillations divided by the number of bunches, one obtains this average bunch phase FFT spectrum. Between 250 GeV and 350 GeV it shows a strong line at 50 Hz. (26. February 2003 06:53:48 PM)

By accelerating protons with AM and Phase Loop II, we reduce on the one hand the longitudinal emittance to about 50% of its normal value of 280 meVs. But, on the other hand, compared to the emittance at injection, it still increases from typically 50 meVs to 130 meVs. Hence, there are still emittance diluting effects during acceleration. Analyzing ramps with AM on, one finds in the FLD beam spectrum a relatively strong line near the mains frequency of 50 Hz between 250 GeV and 350 GeV, see figure 4.16. At these energies, the synchrotron frequency is near 50 Hz, so that the beam is sensitive to external excitation at this frequency. We will discuss the change of the synchrotron frequency during acceleration in chapter 5.

4.3.4 Actual limits of the direct RF amplitude modulation

The method worked without problem at all ramps of beam currents up to 32 mA in 180 bunches. During two ramps with beam current of about 48 mA in 180 bunches, we suppressed all coupled bunch oscillations up to 915 GeV. But unfortunately, before reaching 920 GeV the beam became unstable and the bunches long. A ramp of 52 mA in 120 bunches in three trains, as shown for example in figure 4.6, with AM and Phase Loop II resulted in short bunches without instabilities. This observation should be explained by the fact, that gaps in the occupation pattern result in a more stable behavior [16].

4.4 RF Setting at High Energy

After reaching short bunches at high energy, the next task is to keep them as short as possible during luminosity operation. As already mentioned in section 3.4, the second 52 MHz cavity shows a line at about 28 Hz in the RF frequency spectrum. As the synchrotron frequency is near 30 Hz at high energy, the question arose whether this 'noise' leads to emittance dilution during long storage times. To verify that, we kept the sum voltage of both 52 MHz cavities at

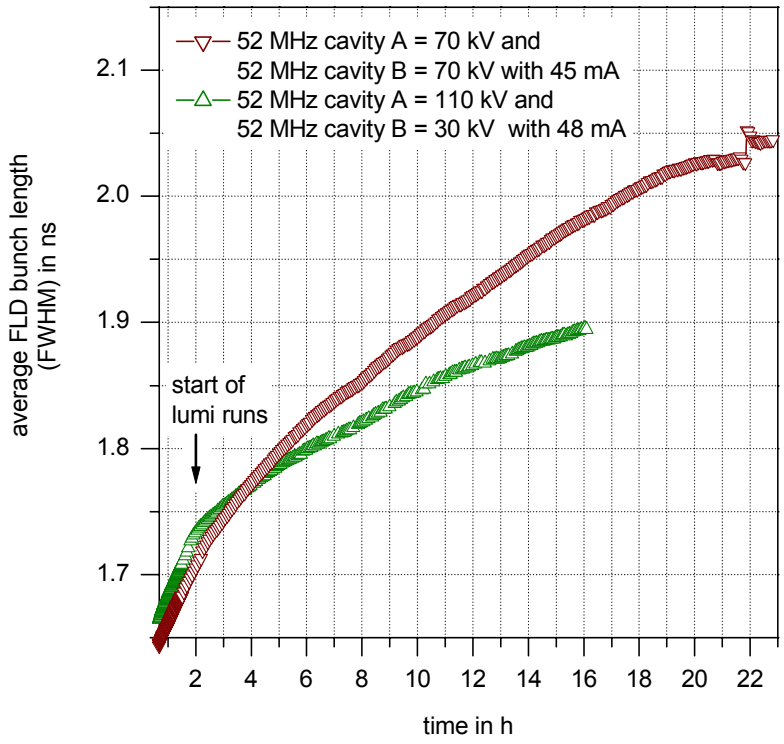

Figure 4.17: Two nearly similar luminosity runs (15. February and 16. February 2003) with equal 52 MHz sum voltages at high energy. A reduced voltage in the 52 MHz cavity B resulted in a significant smaller bunch lengthening rate.

140 kV during two luminosity runs with equal conditions in beam current, initial bunch length etc. During one run, the 52 MHz voltage was provided by equal voltages in both cavities. This was the normal case until then. During the other run, the voltage of the second 52 MHz cavity was reduced to 30 kV, and the first one increased to 110 kV. On the assumption that the 28 Hz line in the second 52 MHz cavity scales with the cavity voltage, we expected to see a difference in the bunch lengthening, taking pace during several hours at luminosity operation.

Figure 4.17 shows the result of this examination. Before the start of luminosity operation, both runs shows nearly similar bunch lengthening rates. After bringing both beams into collision, a significant difference in the bunch lengthening is visible. To first order, the run with the 70 kV in both cavities, shows a bunch lengthening of 17 ps/h. In contrast, the run with reduced voltage in the second 52 MHz cavity shows a bunch lengthening of 11 ps/h. This is a reduction by 35%. Of course, one measurement alone could be a lucky shot. But, after solving the problem with the second 52 MHz cavity in the shut down, we should measure a bunch lengthening equal or smaller than 11 ps/h at beam currents of 48 mA.

The 52 MHz cavities in the HERA proton ring are supplied with ferrite tuners [3]. Cavities with such tuners produce in principle more RF noise as compared to cavities with plunger tuners [17]. To keep this noise component as low as possible, we operated HERA at high energy with 30 kV in each of the 52 MHz cavities, until the end of the run period.

5 Continue Fighting the Blow Up

In this chapter, we will discuss further measures for preserving the longitudinal emittance in the HERA proton ring. In view of the actual schedule to operate HERA II until January 2007, we will only consider measures, which appear feasible before this deadline. In case of an approval of HERA III [18], implying HERA operation after January 2007, some additional measures would become noteworthy.

5.1 Further Debugging HERA Longitudinally

During the shutdown, taking place from March to July 2003, examinations of the 52 MHz cavity B and the accompanying control loops are planned to identify the source of the 28 Hz line in the spectrum. At the moment we are speculating on several possibilities, for example, malfunctions of the control loop power supplies or mechanical resonances.

The Phase Loop I should damp emittance diluting oscillations with $l \leq 22$ perfectly, during injection and acceleration. As the loop damps only oscillation amplitudes larger than 2°, we have first to examine the sensitivity of its beam phase oscillation detector. This detector has probably to be replaced by a more sensitive one. Furthermore, the remote control access to the loop parameters has to be replaced by a reliable one. This is essential to adjust loop parameters in dependence on the changing synchrotron frequency during acceleration. In the next section, we will see that the synchrotron frequency changes from about 30 Hz at injection to 65 Hz at 110 GeV and back to 35 Hz at high energy. A fixed adjustment of the loop parameters for damping synchrotron oscillations with 30 Hz would anti-damp oscillations with 60 Hz.

For a more exact adjustment of the cavity voltage ramp tables, an improvement of the cavity field calibration is advisable. This could be achieved by measuring the synchrotron frequency in dependence on different cavity voltage settings and correlating the results. At a constant energy, RF kicks could excite synchrotron oscillations which are then measured by the FLD.

All possible sources, responsible for exciting the beam with the mains frequency (50 Hz) should be eliminated. This may result in some work.

5.2 Examinations of new RF Voltage Ramp-Tables

In this report, we discussed some examinations, to improve the RF settings. We have to continue these activities.

During injection, we found that additional 208 MHz voltage introduces Landau damping, keeping the bunches short. In principle, it would be wise, to use this possibility and to try some fine tuning.

At about 300 GeV we observed the mains frequency on the FLD beam data. Figure 5.1 shows the synchrotron frequency during acceleration, calculated from the values given in the RF ramp tables. The synchrotron frequency crosses the mains frequency twice. The crossing at 82 Hz was not visible at the recorded FLD until now. This might be an indication, that this crossing is fast enough and causes no problems. But the crossing at 327 GeV is already visible at 250 GeV up to 350 GeV. Hence, we have to think of changing the RF ramp tables in this energy region, for achieving a faster crossing of the mains frequency. Another option would

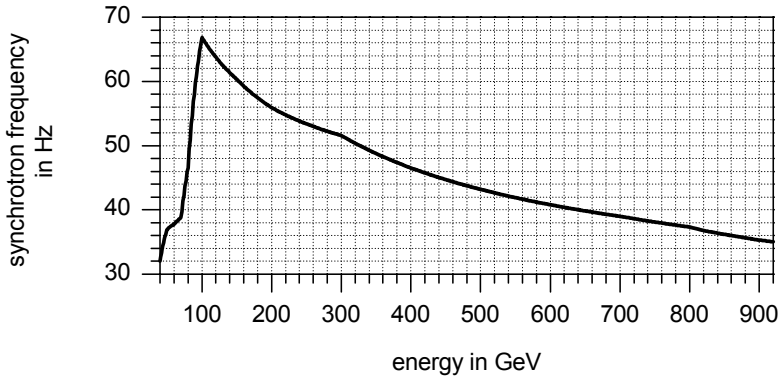

Figure 5.1: Synchrotron frequency during acceleration, calculated from the given RF ramp table values.

be the operation of the HERA proton ring with a synchrotron frequency above 50 Hz at high energy. But, unfortunately the RF voltages required are not available because of limitations at the 208 MHz RF couplers [19].

As already mentioned, the ferrite tuners of the 52 MHz RF cavities produce more RF noise than cavities with plunger tuners [17]. Hence, we have to examine whether an early reduction of the 52 MHz voltage during acceleration is recommended.

5.3 Amplitude-Modulation as a Standard Device

We showed, that the AM of two 208 MHz cavities is sufficient to suppress the coupled bunch instabilities up to at least 32 mA beam current in 180 bunches. For fill patterns with 120 bunches in three trains, we found no upper limit for the beam current until now. By modulating all four cavities, the acceleration of design beam currents of 100 mA in 180 bunches without instabilities should be possible.

The method can be improved by replacing the actual test setup with the function generator by IQ driver boards. Such boards are already in development at the TTF [20]. They output subsequent voltages via DACs, whereas the voltage values are stored in programmable tables. External trigger and clock inputs allow the synchronization of the output voltages with an external timing. With these boards, we are able to program individual I and Q cavity steering signals for each bucket position.

By modulating the amplitude of the steering signals, one always influences the phasing, because the cavities and their controls show deviations from the ideal behavior. Such effects can be taken into consideration and corrected easily by adjusting the IQ tables.

For standard operation, the AM should be switched on automatically during acceleration, via a ramp table or the HERA sequencer. As the parallel operation of Phase Loop II is essential, this loop has to observe itself, whether the synchronization for injection or between the proton and electron ring is in the lock process. In this case, the phase loop has automatically to take care, that this lock processes are not negative influenced by its correction values. As final goal, the phase loop II and AM should automatically start operation without explicit requests from operators and cause no negative influence on the remaining operation. It should also be possible to switch them off for particular cases.

To prove that luminosity gain is achieved by the method, we have to perform measurements of the transversal beam dimensions. Furthermore, the influence of the AM on the reliability

of the final stage amplifiers and the cavity control systems has to be monitored, because of the increased demand of RF power.

5.4 Further Development of the FLD

Some essential work has still to be done at the FLD. This is first of all the automatic reading of the data stored at the dCache. At the moment, this data has to be copied by hand with several UNIX commands before the analysis can take place.

For future RF noise studies, the single bunch measurement has to be commissioned. With this measurement, we will be able to record the bunch data of single bunches for time intervals of up to 70 sec without gaps. Thus providing a solid basis for determinations of the beam spectrum with high resolution or sensitivity.

The actual bunch length measurement fits in principle a Gaussian to the bunch shape at two points, by measuring the 52 MHz and the 208 MHz bunch Fourier component. As long as the bunch populations show similar distribution, this is sufficient. But unfortunately, coupled bunch oscillations tend to change the population at the bunch tails. This has an influence on the resulting FLD bunch length. Figure 5.2 shows the same bunch during acceleration, once before a coupled bunch oscillation and once afterwards. From the bunch shape, we determine

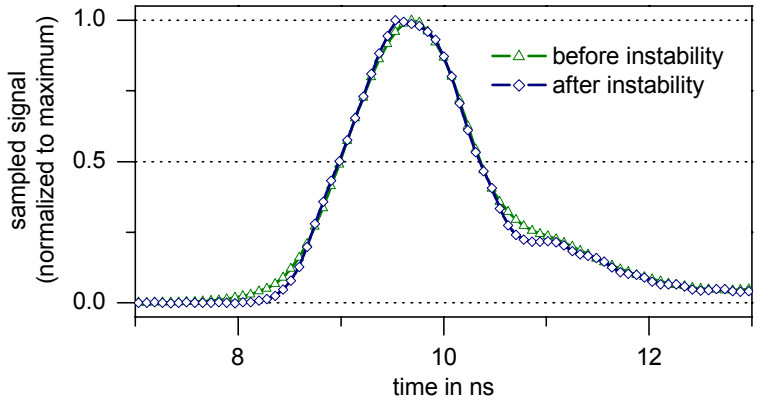

Figure 5.2: Bunch shape of bunch no 5, before (170 GeV) and after (820 GeV) a coupled bunch instability with equal FWHM value. Data from 24th February 06:20:44 PM and 06:36:29 PM.

the same FWHM bunch length of 1.36 ns, but the FLD bunch length is first 1.63 ns and then 1.52 ns. Both values are too large. To calculate the emittance values, presented in this report, all FLD bunch lengths were re-scaled by comparing FLD values with the values obtained form the bunch shape measurements (CMFL). The re-scaling was the same for all values measured before an instability. Separately, one had to choose another re-scaling for all the values measured afterwards. To improve the bunch length diagnostics if the FLD it is advisable to implement additional filter frequencies. That mean, to measure for example in addition to the 52 MHz and 208 MHz bunch Fourier components, the 78 MHz, 104 MHz, 130 MHz, 156 MHz and 182 MHz bunch Fourier components. Then an algorithm, calculating the bunch length from the Fourier components, would be able to consider different bunch shapes.

The FLD records presented, showing injections, were taken arbitrarily. If the FLD takes a data record every 11 sec with a length of 2.3 sec, one has a probability of 21 % to record an injection. The FLD timing system also offers some unused features to trigger on injections. Using them would result in a more systematic recording and examination of injection process.

5.5 Further Measures

For systematic and precise examination of the coasting beam production and its causes, the use of data, obtainable from the Very Forward Proton Spectrometer (VFPS) of the H1 experiment [21], could be very useful. Initially one would record the rate and energy of the particles hitting the VFPS within the dump gap [22]. There are no colliding and no pilot bunches in the dump gap, so we expect to measure particles resulting from coasting beam.

Finally, two further measures appear to be realizable within the HERA II run until January 2007, provided one starts the implementation immediately: The first is the implementation of an RF feed forward, to decrease the effective cavity impedances seen by the beam. The second one is an one turn delay feedback, as implemented in the CERN SPS. We will not go into the details here. As an example, a short description of the principles can be found in [23]. For good maintenance, such loops should be realized by using DSPs (digital signal processors) or FPGAs (field programmable gate arrays).

6 Conclusion

The Fast Longitudinal Diagnostics system (FLD) have become a standard tool for examination of the longitudinal stability in the HERA proton ring. Some remaining things have to be debugged and the automatic reading of dCache data must be implemented. Provided that this work is done as enthusiastically as in the past, it should be finished before the restart of HERA in July 2003.

We debugged the Phase Loop II, so that it damps perfect beam oscillations of the coupled bunch mode $l = 0$ at injection, during acceleration and at high energy. Supervision routines have to be implemented in future, to prevent automatically negative interferences with synchronization loops. Phase Loop I requires more attention. The sensitivity has to be increased, so that beam oscillations with amplitudes larger than 0.2° can be damped, instead of only 2°. Then it will be able to damp the coupled bunch modes with $l \leq 22$. Furthermore, the remote control of the parameters must be made robust. If the loop is in operation, a break down of the remote control would immediately cause beam loss.

In the last HERA run period, we showed, that an amplitude modulation of the 208 MHz RF voltage in combination with the Phase Loop II is sufficient to prevent coupled bunch oscillations reliably at beams with more than 32 mA in 180 bunches. For beams with more than 50 mA in 120 bunches, distributed over three trains, we no longer observed coupled bunch instabilities when the AM and the Phase Loop II were in operation. We obtained a reduction of the longitudinal FWHM emittances from values greater than 280 meVs down to typical values of 120 meVs at high energy. This corresponds to a bunch length reduction from 1.51 ns down to 0.98 ns. As soon as IQ driver boards for VME crates are available, the AM will be implemented as a automatically working standard device. By modulating the voltages of all four cavities instead of two, we expect, that we can also suppress coupled bunch oscillations for proton beams with 100 mA in 180 bunches.

At injection energies, we found that a 208 MHz sum voltage, with a value of 1/4 of the 52 MHz sum voltage, result in an enormous reduction of the bunch lengthening, caused by transient beam loading. Furthermore we found 50 Hz excitations of the beam between 250 GeV and 350 GeV. Future RF ramp tables will have to consider such facts. Hence, finding more precise RF calibrations is recommended.

Examinations of the RF noise behavior of the cavities, first carried out by S. Ivanov and O. Lebedev from IHEP, showed a prominent line at 28 Hz in the FFT spectrum of the 52 MHz cavity B. We assume that this causes the beam oscillations observed at injection up to 70 GeV. By reducing the nominal RF voltage of this cavity at high energy, we found a reduction of the bunch lengthening at luminosity operation of 35%. Until the HERA restart in July, some studies of this cavity and its RF control will be undertaken, to eliminate this effect.

Emittance diluting effects during luminosity operation are also expected to be one of the causes for coasting beam. To establish connections between technical malfunctions, emittance diluting effects and the coasting beam production rate, we have first to set up systematic examinations. Using data obtained by the H1 VFPS in the dump gap is promising on that score.

Summarizing: the results achieved make one quite confident that the longitudinal emittance of the HERA proton ring can be controlled and further reduced in the future.

Appendix

A.1 Amplitude Modulation due to $h+1$ Cavity

At the HERA proton ring, the use of the harmonic number $h+1 = 4401$ for one of the 208 MHz cavities would cause a frequency change of its drive signal by the revolution frequency. We expect that the cavity controls will tolerate such a frequency change without technical modifications.

For the estimation of the net voltage, seen by a bunch at bucket j, we proceed in the following way: Normally, the RF voltage at a storage ring is given by

$$v_h(t) = V_h\, e^{i\,\omega_{RF}\,t} \tag{A.1}$$

with

$$\omega_{RF}\,t = 2\,\pi\,\frac{h}{M}\,j, \tag{A.2}$$

where M is the number of buckets. The voltage of a cavity operated with the harmonic number $h+1$ has the voltage

$$v_{h+1}(t) = V_{h+1}\, e^{i\,\omega_{RF}\,\frac{h+1}{h}\,t}. \tag{A.3}$$

Hence, we get, for the bucket position j, the net RF voltage of

$$V(j) = V_h\, e^{i\,2\,\pi\,\frac{h}{M}\,j} + V_{h+1}\, e^{i\,\frac{h+1}{h}\,2\,\pi\,\frac{h}{M}\,j} \tag{A.4}$$

resulting in the RF amplitude

$$|V(j)| = V_h \sqrt{1 + \left(\frac{V_{h+1}}{V_h}\right)^2 + 2\,\frac{V_{h+1}}{V_h}\,\cos\left(\frac{2\,j\,\pi}{M}\right)}\,. \tag{A.5}$$

For the estimation of the coherent synchrotron frequency spread, introduced by the modulated RF voltage, we use the relation between synchrotron frequency and RF voltage

$$f_{s0} = \sqrt{V_h}\,. \tag{A.6}$$

The frequency spread is then given by

$$\frac{S_f}{f_{s0}} = \sqrt{\sum_{j=0}^{M-1}\left(\frac{f_s(j)}{f_{s0}} - 1\right)^2}\,, \tag{A.7}$$

with

$$\frac{f_s(j)}{f_{s0}} = \frac{\sqrt{|V(j)|}}{\sqrt{V_h}}\,. \tag{A.8}$$

By carrying out the summation by using a computer algebra system like *Mathematica* we obtain for HERA ($M = 220$) and $0 \leq V_{h+1} \leqslant V_h$ in good approximation

$$\frac{S_f}{f_{s0}} \approx 5\,\frac{V_{h+1}}{V_h} \qquad \text{for} \quad \frac{V_{h+1}}{V_h} \leq 1. \tag{A.9}$$

A disadvantage of this method is a systematic shift of the bunch to bunch spacing over all bunches. This means, the bunch centroid of bunch j is shifted in dependence on the ratio of the voltages $\frac{V_{h+1}}{V_h}$ by

$$\Delta\phi = \arctan\frac{\mathrm{Re}\;V\,(j)}{\mathrm{Im}\;V\,(j)} = \frac{\cos\left(\frac{2\,\pi\,h\,j}{M}\right) + \frac{V_{h+1}}{V_h}\cos\left(\frac{2\,\pi\,(h+1)\,j}{M}\right)}{\sin\left(\frac{2\,\pi\,h\,j}{M}\right) + \frac{V_{h+1}}{V_h}\sin\left(\frac{2\,\pi\,(h+1)\,j}{M}\right)}\,. \tag{A.10}$$

A.2 Direct RF Amplitude Modulation

Following the procedure of section A.1, a sinusoidal modulation of the RF amplitude with the revolution frequency, will provide a bunch at bucket j with a voltage of

$$V_{\mathrm{amp}}\,(j) = V_0\left(1 + \frac{V_{\mathrm{mod}}}{V_0}\cos\left(\frac{2\,\pi\,j}{M}\right)\right), \tag{A.11}$$

where V_0 is the RF voltage without modulation and V_{mod} the modulation amplitude. This modifies the synchrotron frequency as follows

$$\frac{f_s\,(j)}{f_{s0}} = \frac{\sqrt{V_{\mathrm{amp}}\,(j)}}{\sqrt{V_0}} = \sqrt{1 + \frac{V_{\mathrm{mod}}}{V_0}\cos\left(\frac{2\,\pi\,j}{M}\right)}\;. \tag{A.12}$$

Using (A.7) for $M = 220$, we obtain the bunch to bunch frequency spread in dependence on

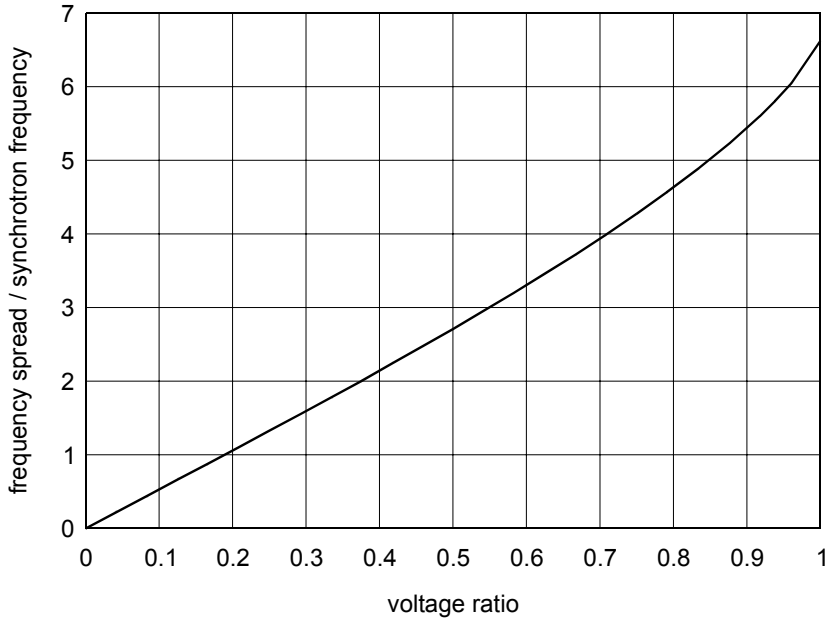

Figure A.1: Synchrotron frequency spread due to a sinusoidal RF amplitude modulation with the revolution frequency.

the voltage ratio, as shown in figure A.1. For voltage ratios below 0.6, we obtain the same approximation as in the $h + 1$ case:

$$\frac{S_f}{f_{s0}} \approx 5\,\frac{V_{\mathrm{mod}}}{V_0} \qquad \text{for} \quad \frac{V_{\mathrm{mod}}}{V_0} < 0.6 \tag{A.13}$$

Bibliography

[1] M. A. Furman, 'The hourglass reduction factor for asymmetric colliders', Asymmetric B-Factory collider Note No. SLAC-ABC-41-REV (1991)

[2] personal communication with G. H. Hoffstaetter, DESY (2001)

[3] E. Vogel, 'Fast Longitudinal Diagnostics for the HERA Proton Ring', Ph.D. Thesis, University of Hamburg, DESY Report DESY-THESIS-2002-010 (2002); http://www-library.desy.de/diss02.html

[4] http://desyntwww.desy.de/tine

[5] J. Andruszkow, P. Jurkiewicz, F. Tonisch, '8-channel FastADC with 14 bit resolution', tesla.desy.de/doocs/hardware/8ch_10MHz_ADC_manual.pdf (2001)

[6] http://www-dcache.desy.de/

[7] W. Kriens, 'PETRA Bunch Rotation', in *Proceedings of the Particle Accelerator Conference, Vancouver, Canada,* 1997

[8] personal communication with S. Ivanov and O. Lebedev from IHEP, DESY (2002)

[9] S. Ivanov, O. Lebedev, 'Noise Performance Studies at the HERA-p Ring ', DESY Report No. DESY-HERA-03-02 (2003)

[10] E. Vogel, 'Examination of the Longitudinal Stability of the HERA Proton Ring', Eighth European Particle Accelerator Conference (EPAC'02), Paris, 3-7 June 2002; http://accelconf.web.cern.ch/AccelConf/e02/KEYWORDS/K022.htm

[11] personal communication with T. Bohl, CERN (2002)

[12] T. Bohl, T. Linnecar, E. Shaposhnikova and J. Tuckmantel, 'Study of Different Operating Modes of the 4th RF Harmonic Landau Damping System in the CERN SPS', in *Proceedings of the European Particle Accelerator Conference, Stockholm, Sweden,* 1998 (CERN Report No. SL-98-026 RF, 1998)

[13] S. A. Bogacz, S. Stahl, 'Coupled Bunch Instability in Fermilab Booster - Longitudinal Phase-Space Simulation', Fermi National Accelerator Laboratory Report FERMILAB-Conf-88/65 (1988); http://fnalpubs.fnal.gov/archive/1988/conf/Conf-88-065.pdf

[14] F. J. Sacherer, 'A longitudinal stability criterion for bunched beams', to be presented to the *1973 Particle Accelerator Conference San Fransisco*, 5-7 March 1973 (CERN Report No. CERN-MPS-Int. BR-73-3, 16. February 1973)

[15] personal communication with G. Hoffstaetter, he calculated this value, DESY (2001)

[16] R. D. Kohaupt, 'On Multi-Bunch Instabilities for Fractionally Filled Rings', DESY Report No. DESY M 85-139 (December 1985)

[17] personal communication with S. Ivanov from IHEP, DESY (2003)

[18] Letters of Intent for HERA III Programme, April, 2003;
http://wwwhera-b.mppmu.mpg.de/hera-3/

[19] personal communication with R. Wagner, DESY (2003)

[20] personal communication with S. Simrock, DESY (2003)

[21] P. Van Mechelen, 'A Very Forward Proton Spectrometer for H1', Talk presented at LISHEP 2002, Session C: Workshop on Diffractive Physics, February 4-8, 2002 Rio de Janeiro, RJ, Brazil (2002); hep-ex/0203029

[22] personal communication with D. Pitzl from H1, HERA Betriebsseminar in Salzau, 05-08 May 2003

[23] D. Boussard, G. Lambert, T.P.R. Linnecar, 'Improved Impedance Reduction in the CERN SPS Superconducting Cavities for High Intensity Proton Operation', Fifteenth Particle Accelerator Conference (PAC 1993), Washington, D.C., 17-20 May 1993

Acknowledgments

I would like to thank Dr. Ferdinand Willeke, for his continuous interest and support. He gave the permission to perform these studies parasitically to normal storage ring operation. This opportunity for performing studies continuously was essential to obtain experience with the measures taken and to improve the procedures.

I want to express my gratitude to Hong Gong Wu. He programs the FLD-servers, supplying the pre-possessed data. This is a sophisticated task, due to the large amount of data involved. There were many fruitful discussions about the best way to take and supply the data to the accelerator control system.

I would also like to thank Victor Soloviev. He is responsible for the implementation of the FLD data display program. It is his achievement, that the FLD data is visualized and can be analyzed in a convenient way.

I offer my thanks to Josef Wilgen, for his support in getting familiar with the dCache system, required for storing the FLD data permanently.

With sincerest appreciation, I would also like to mention Wilhelm Kriens, Uwe Hurdelbrink and Kai Brede. They were always open and helpful to set up particular hardware, for example they provided the functional generator together with its remote control for the RF amplitude modulation. Furthermore, they fixed bugs in the RF generation.

Many people were additionally involved in the final development period of the FLD and activities concerning the proton RF. It is not possible to do justice to all of them, but I would particularly like to thank Dr. Stefan Choroba, Dr. Reinhard Bacher, Bernd Closius, Philip Duval, Olaf Hensler, Steve Herb, Gerd Hochweller, Serguei Ivanov, Oleg Lebedev, Kay Rehlich, Dr. Stefan Simrock, Andreas Sommer, Frank Tonisch and Richard Wagner.

I would like to thank all my colleagues from the MPY group for providing a stimulating and friendly work environment.

I offer my thanks to Dr. John Maidment, Susan Wipf for reading parts of this report.

Last but not least, I would like to thank Dr. Markus Hoffmann and Dr. Mathias Vogt for their willingness to look after the HERA proton FLD in future.